ION FORMATION IN MALDI MASS SPECTROMETRY

Renato Zenobi and Richard Knochenmuss
Department of Chemistry, Swiss Federal Institute of Technology (ETH), Zürich, Switzerland

Received 4 September 1998; revised 12 November 1998; accepted 12 November 1998

The origin of ions in matrix-assisted laser desorption/ionization (MALDI) mass spectrometry is currently a matter of active research. A number of chemical and physical pathways have been suggested for MALDI ion formation, including gas-phase photoionization, ion–molecule reactions, disproportionation, excited-state proton transfer, energy pooling, thermal ionization, and desorption of preformed ions. These pathways and others are critically reviewed, and their varying roles in the wide variety of MALDI experiments are discussed. An understanding of ionization pathways should help to maximize ion yields, control analyte charge states and fragmentation, and gain access to new classes of analytes. Mass Spec Rev 17: 337–366, 1998
Keywords: *MALDI mass spectrometry; ion formation; proton transfer*

Contract grant sponsor: Kommission für Technologie und Innovation
Contract grant no.: 3165.1

Contract grant sponsor: ETH
Contract grant number: TH 0-20-402-97

CCC 0277-7037/99/050337-30

I. INTRODUCTION

Matrix-assisted Laser Desorption/Ionization (Karas et al., 1985; 1987; Karas & Hillenkamp, 1988; Tanaka et al., 1988; Hillenkamp et al., 1991), along with electrospray ionization, is now among the most important ionization methods for nonvolatile, high molecular weight compounds (Overberg et al., 1992; Caprioli et al., 1996; Chapman, 1996). MALDI is widely used for mass spectrometric analysis of large, nonvolatile biomolecules, in particular peptides, proteins, oligonucleotides, and oligosaccharides. Synthetic polymers of high molecular weight are also studied by MALDI-MS, with respect to their oligomer spacing, end-group distribution, molecular weight distribution, and polydispersity. MALDI has also been successfully used for the investigation of fullerenes, fullerene derivatives, and synthetically prepared dendrimers. It has even been shown that MALDI can, under certain conditions, be used for the study of weakly bound noncovalent complexes. High-molecular-weight environmental materials such as kerogens, coal tars, humic acids, and fulvic acids are also being studied with MALDI or related techniques. Despite this impressive range of applications, the nature of the ionization process remained poorly understood until recently. Over the last couple of years, we have witnessed a wave of new experiments, new data, and new ideas aimed at explaining the MALDI ionization process. We, therefore, feel that it is timely to present a review on this topic.

A better understanding of the ionization process in MALDI is important for several reasons: to improve ion yields, to better control fragmentation, to control the charge state, and to gain access to new classes of compounds by MALDI. Enhanced knowledge of the ion formation process could provide rational guidelines for matrix selection for a given analytical problem. It could pinpoint possible reasons for discrimination effects in quantitative MALDI experiments.

One of the major reasons why it is difficult to understand MALDI ionization is that, very probably, no single mechanism can explain all ions observed, even in a single MALDI experiment. In addition, the general concept of MALDI encompasses a great variety of experimental conditions, including different laser wavelengths, pulse energies and lengths, and different sample preparation methods. The mass spectrum can be recorded either in the positive or negative ion mode. There are many different classes of analyte molecules, many different MALDI matrices or comatrices, and even more matrix-analyte combinations. All these parameters affect the mass spectrum through the ion formation process. Furthermore, the overall ion-to-neutral ratio in (UV) MALDI experiments is only about 10^{-4} (Mowry & Johnston, 1994; Puretzky & Geohegan, 1997), i.e., we are trying to describe and understand mechanisms leading to *minority* species in the process. Here, we will focus on ionization processes that relate to typical MALDI experiments, such as the detection of a protein in its singly protonated form. We will also emphasize cases where the mechanistic aspects are particularly clear; e.g., transition metal cationization of polystyrene. And finally, we will make a special effort to deduce rules and guidelines that will be of practical value to the MALDI user.

Ionization processes occurring in MALDI mass spectrometry have not previously been the object of a review, though the topic has fascinated many authors and is frequently mentioned in MALDI articles. MALDI developed from laser desorption techniques without matrix, as did mechanistic thinking about it. In 1985, for example, Karas, Bachmann, and Hillenkamp (Karas et al., 1985) discussed laser desorption ionization mechanisms in films of UV-absorbing amino acids. These materials were effectively MALDI matrices, and the ideas presented carried through into work on MALDI ionization. Among the more extensive later discussions are the 1992 article by Ehring, Karas, and Hillenkamp (Ehring et al., 1992), and the 1995 work of Liao and Allison (Liao & Allison, 1995). Both of these works treated a large number of possible ionization routes, then focused on ionization of peptides, due to the great importance of that application of MALDI. The 1996 book by Standing and Ens (Standing & Ens, 1996) also includes mechanistic aspects of ion formation.

The MALDI ionization process bears some similarity to that of secondary ion mass spectrometry (SIMS) and fast atom bombardment (FAB) (Szekely, 1997); that topic has been comprehensively reviewed by Sunner (Sunner, 1993). In an interesting bit of reverse influence, there has even been a recent suggestion to use MALDI matrices to enhance the ion yield in static SIMS (Wu & Odom, 1996).

Much more research has been devoted to studying the desorption/ablation process in MALDI (Vertes et al., 1993; Johnson, 1994), and it can be considered to be fairly well understood. The MALDI plume is commonly compared to a pulsed jet expansion or to pulsed hydrodynamic flow. Plume dynamics have some relevance to the formation of ions, and are briefly summarized in Section III.B.

This review is organized in the following manner. Section II describes some available experimental parameters, with an emphasis on those that are thought to teach us something about ionization mechanisms. Section III.A presents mechanisms for formation of primary charges in the MALDI plume, and Section III.B discusses secondary reactions that lead to the observed ions. The reader who is more interested in practical aspects of MALDI can directly turn to Section IV, where the mechanisms are summarized in two tables. Finally, concepts that are of direct practical relevance for the design of MALDI experiments are derived from the mechanistic considerations.

TABLE 1. Laser wavelengths, pulse widths, and corresponding photon energies.

Laser	Wavelength	Photon energy (kcal/mol)	Photon energy (eV)	Pulse width
Nitrogen	337 nm	85	3.68	<1 ns − few ns
Nd:YAG × 3	355 nm	80	3.49	typ. 5 ns
Nd:YAG × 4	266 nm	107	4.66	typ. 5 ns
Excimer (XeCl)	308 nm	93	4.02	typ. 25 ns
Excimer (KrF)	248 nm	115	5.00	typ. 25 ns
Excimer (ArF)	193 nm	148	6.42	typ. 15 ns
Er:YAG	2.94 μm	9.7	0.42	85 ns
CO_2	10.6 μm	2.7	0.12	100 ns + 1 μs tail

II. EXPERIMENTAL PARAMETERS IN MALDI-MS

A major obstacle to the elucidation of ion formation mechanisms in MALDI has been that the range of samples, matrices, and experimental parameters is enormous. In addition, different mass analyzers with different observation time scales, acceleration fields, sample temperatures, incident angles of the laser beam, laser wavelengths, pulse energies, and pulse widths are used; these parameters can all influence the outcome of the MALDI mass spectrum. Here we discuss but a few of these parameters that we believe are decisive for ion formation.

A. Laser Wavelength

The laser wavelength is a particularly important parameter in MALDI. The most frequently used wavelength is 337 nm from the nitrogen laser, but harmonics of the Nd:YAG laser fundamental, various excimer laser lines, and, more recently, radiation from infrared lasers such as Er:YAG lasers or carbon dioxide lasers are also employed. Table 1 gives the wavelengths and the corresponding photon energies for these laser sources; typical pulse widths are also indicated. Tunable lasers, such as dye lasers, optical parametric oscillators, and free electron lasers are not included in the table; their use in MALDI remains limited to specialized research purposes.

An interesting observation is that MALDI mass spectra obtained with UV and IR laser wavelengths look similar (Fig. 1) (Niu et al., 1998). However, there are higher pulse energy requirements in IR MALDI due to lower matrix absorption, and the sample consumption is accordingly higher (Berkenkamp et al., 1997; Niu et al., 1998). A greater tendency to form multiply charged high-mass ions, less metastable fragmentation, and adduct formation have also been reported for IR MALDI (Overberg et al., 1990; 1991; Berkenkamp et al., 1998; Zhang et al., 1998).

B. Laser Pulse Width

The influence of the laser pulse width has also been investigated, but was found to have little or no influence on MALDI mass spectra, at least up to pulse lengths of tens of nanoseconds from commonly available laser sources (Chevrier & Cotter, 1991; Beavis, 1992; Demirev et al., 1992; Johnson, 1994; Riahi et al., 1994; Dreisewerd et al., 1995; 1996). This factor indicates that the desorption/ionization process is determined by the energy density supplied to the sample by the laser pulse (fluence, J/cm^2), rather than by the rate of energy flow (irradiance, W/cm^2). As will be discussed later, this difference has important consequences for mechanistic models.

C. Matrices

The choice of matrix is crucial for success in MALDI experiments. Most frequently, analyte is co-crystallized with an excess of a solid matrix material. Figure 2 gives the structures of frequently used MALDI matrices, their chemical names, trivial names, and abbreviations. We will usually use abbreviations in the following text. A more complete list of MALDI matrices can be found on the "matrix depot" internet site (Rockefeller University).

Derivatives of benzoic acid, cinnamic acid, and related aromatic compounds were recognized early on as good MALDI matrices for proteins (Beavis & Chait, 1989). Juhasz et al. introduced HABA as a matrix for peptides, proteins, and glycoproteins up to 250 kDa (Juhasz et al., 1993). For oligonucleotides, 3-HPA (Wu et al., 1993; 1994), glycerol (Berkenkamp et al., 1998), and succinic acid (Nordhoff et al., 1993) are used as matrices in the UV and in the infrared, respectively. Many common UV matrices work well in the infrared, too (Overberg et al., 1992). By far, not all matrices are carboxylic acids. For example, 2,4,6-trihydroxy acetophenone (Pieles et al., 1993) has been shown to be useful for studying oligonucleotides, 3-aminoquinoline is a good matrix for polysaccharides (Metzger et al., 1994), and the laser dye coumarin 120 has been found useful in MALDI MS of monosulfated oligosaccharides (Dai et al., 1997). Fitzgerald et al. (Fitzgerald et al., 1993) introduced a number of basic matrices derived from substituted pyrimidines, pyridines, and anilines, for example, para-nitroaniline. Some of these matrices have proven to be excellent for observing

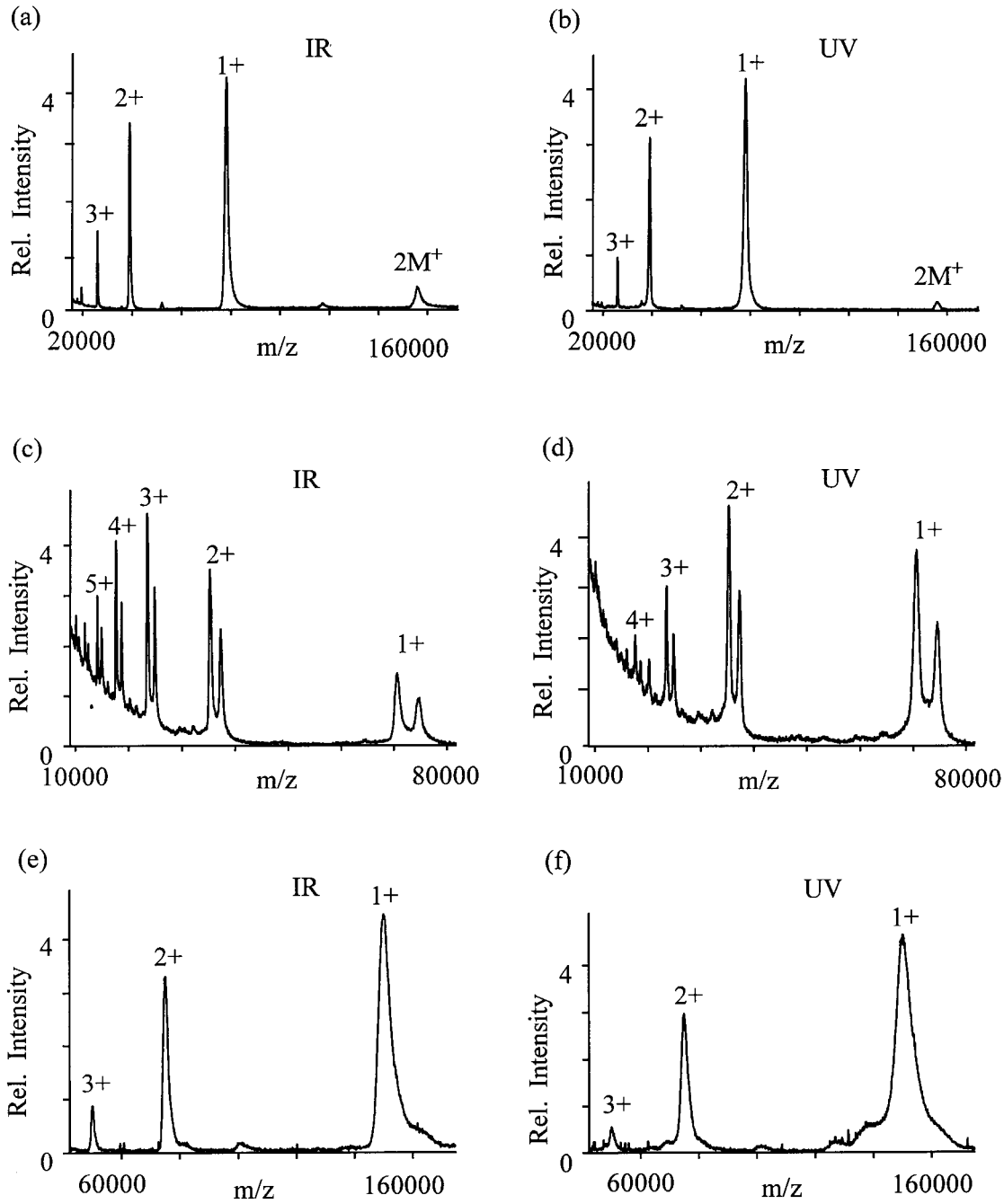

FIGURE 1. IR- and UV-MALDI spectra of three high mass proteins: transferrin, synapsin, and IgG in sinapic acid. (a) IR-MALDI of transferrin; (b) UV-MALDI of transferrin; (c) IR-MALDI of synapsin; (d) UV-MALDI of synapsin; (e) IR-MALDI of IgG; and (f) UV-MALDI of IgG. (Reprinted by permission of Elsevier Science from Niu et al., 1998. Copyright 1998 by American Society for Mass Spectrometry.)

noncovalent complexes and supramolecular assemblies, because they allow samples to be prepared under non-denaturing conditions.

MALDI is generally characterized by little prompt fragmentation. Most fragments seem to be generated as the ions pass through the drift tube, by unimolecular (metastable) decomposition and by collisions with the background gas; the overall process is called "post-source decay" (PSD) (Spengler et al., 1992). This also implies that fragmentation is dependent not only on the MALDI process, but also on experimental parameters such as the nature and pressure of the residual gas in the mass spectrometer. Even the extrac-

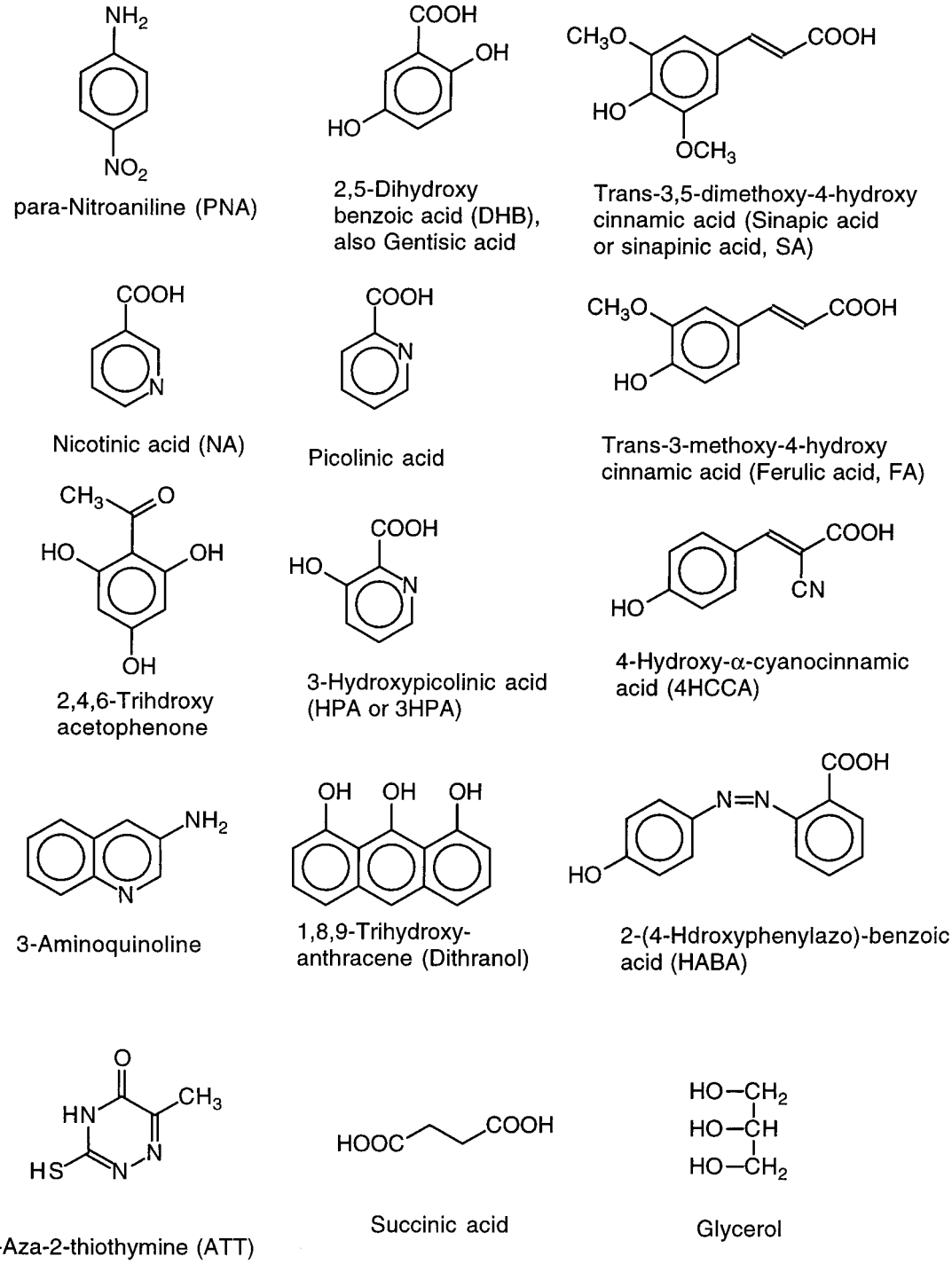

FIGURE 2. Structures, chemical names, trivial names, and abbreviations of frequently used MALDI matrices.

tion field contributes to fragmentation, because ions are pulled through the neutral plume and suffer collisions.

Nevertheless, the choice of matrix is also important for the control of fragmentation. A small number of matrices have been studied with regard to their propensity to induce fragmentation and, thereby, are classified as "hot" or "cold." Karas et al. (Karas et al., 1995) have found that, for protonated glycoproteins, post-source decay decreases in the order SA > DHB > HPA. This order agrees with Spengler et al. (Spengler et al., 1992), who also described SA as a "hotter" matrix than DHB. In MALDI mass spectrometry of oligodeoxynucleotides, DHB has also been found to induce more

fragmentation than 3HPA (Zhu et al., 1995). One proposed explanation for the hot and cold nature of matrices is simply the temperature at which they sublime, and, hence, desorb the analyte (Karas et al., 1996).

A large variety of matrix additives are used, but it would be too complex to systematically discuss all the combinations from a mechanistic viewpoint. Many additives probably function by improving co-crystallization or by sequestering excess salts, rather than by directly affecting ionization. More relevant to this review are liquid matrices and liquid/solid two-phase matrices, which circumvent some of the problems associated with solids, such as the need for co-crystallization or solubility requirements. Liquid matrices can continuously refresh their surfaces, largely eliminating the "hot spot" phenomenon known for solid matrices. UV-absorbing liquids such as 3-nitrobenzyl alcohol or nitrophenyloctylether, as well as IR-absorbing liquid matrices such as glycerol and triethanolamine, have been used to affect UV-MALDI and IR-MALDI, respectively (Karas et al., 1987; Zhao et al., 1991; Chan et al., 1992; Li et al., 1993; Yau et al., 1993; Chan et al., 1994; Williams et al., 1996).

If an absorbing solid material is added to a nonabsorbing liquid, then the advantages of liquid matrices are essentially retained, and the solid can be chosen to absorb the laser wavelength. One of the earliest MALDI experiments that demonstrated the generation of large biomolecular ions was reported by Tanaka et al. in 1988. They used very fine cobalt particles mixed with liquid glycerol (Tanaka et al., 1988). After a long lapse, the method has been revived and extended to include a variety of particulate materials and liquid matrices (Sunner et al., 1995; Dale et al., 1996; Schürenberg, 1996; Dale et al., 1997; Kraft et al., 1998). The technique has been called two-phase MALDI, to differentiate it from the usual methods that utilize solid matrices, or surface-assisted laser desorption/ionization (SALDI). A related method uses solids known as normal MALDI matrices or other UV- or IR-absorbing compounds such as dyes suspended or dissolved in a nonabsorbing liquid (Cornett et al., 1992; 1993; Kolli & Orlando, 1996; Zöllner et al., 1996; 1997; Kolli & Orlando, 1997; Kraft et al., 1998; Sze et al., 1998). Frozen water, water/glycerol, or water/particle mixtures have also been used as an IR MALDI matrix with some success (Becker et al., 1990; Berkenkamp et al., 1996; Hunter et al., 1997; Caldwell & Murray, 1998; Kraft et al., 1998); for example, for the analysis of oligonucleotides.

Unfortunately, there are still no clear guidelines for matrix selection for a particular analytical problem, and better matrices are, therefore, often found only after screening of a large number of candidate compounds (Fitzgerald et al., 1993; Wu et al., 1993). We offer some guidelines below based on ion formation mechanisms, but many of the uncertainties are related to matrix crystallization or analyte incorporation, and require further study.

III. MECHANISMS OF MALDI ION FORMATION

In this section, we present a number of possible ion formation mechanisms. We divide these mechanisms into two categories: primary and secondary. By "primary" ionization, we refer to generation of the first ions from neutral molecules in the sample. These ions are often matrix-derived species. "Secondary" mechanisms are those that lead to ions that are not directly generated by primary processes; in particular, analyte ions. In the mass spectrum, the products of primary and secondary processes are both usually observed. The role of individual mechanisms in different MALDI experiments is summarized in Section IV. In the discussion to follow, matrix molecules are denoted in reaction schemes by M, and analytes by A.

A. Primary Ion Formation

1. Basic Thermodynamics of Ion Formation

Only a few types of ions are commonly observed in MALDI. In the positive mode, these are radical cations, protonated pseudo-molecular ions, and cationized pseudo-molecular ions in the form of metal ion adducts. Some general remarks about charge separation are helpful for evaluating possible mechanisms. All the energetics discussed below for positive ions apply to negative ions as well.

Consider first the limiting case of the generation of free ions in vacuum from a neutral molecule. This process is highly endothermic, mainly due to the Coulomb attraction of the charges being separated. Although free protons are not observed in MALDI, their creation from the matrix is an important reference value. C—H or O—H bond lengths are short, around 0.1 nm, leading to a high theoretical Coulomb energy cost for generation of $H^+ + R^-$: 14 eV or 322 kcal/mol. Compare this energy with the known value of 14.65 eV for the removal of the proton from the phenol hydroxyl group (Jouvet et al., 1990). Similar energies have been measured for ion pair generation from small hydrogen-containing molecules (Gallagher et al., 1988). The separation of a $Na^+ Cl^-$ ion pair in vacuum, where the initial distance is larger, r =0.3 nm, theoretically costs 4.8 eV or 110 kcal/mol. The binding energy of NaCl in a salt crystal is higher than in the gas phase, by a factor of the Madelung constant, which has the value 1.75 for a bulk NaCl crystal. Extracting the individual ions from within a salt crystal in a MALDI sample, thus, requires $4.8 \times 1.75 = 8.4$ eV. These energies are very significant compared to the photon energy of the usual MALDI nitrogen laser. Generation of a sodium ion should require the direct deposition of 3 photons at one site, and a free proton should cost 4 photons. At laser intensities high enough for this process to be common, extensive analyte fragmentation would also occur. Of

course, it is solvation effects within the MALDI sample that facilitate MALDI ion separation, as discussed next. However, we will come back to these important gas-phase reference energies, because the ions must finally reach this state.

Dielectric screening by residual solvent, matrix, or nonionic parts of large molecules dramatically reduces the Coulomb energy, as do large ionic radii in the case of macromolecular ions. If we assume a bulky, screened ion pair with r = 1 nm and a relative dielectric constant of $\epsilon = 5$, then only 0.28 eV or 6.6 kcal/mol is needed for separation. This value is a serious underestimate, because attractive induction and dispersion forces will be significant in such cases. For example, the ion-dipole energy of Na^+ complexed with a single water molecule is 1 eV or 23 kcal/mol (Israelachvili, 1991). However, screening definitely has an effect even when the environment cannot be considered a continuous classical dielectric. A Coulomb energy for RO-H ionic separation of about 4.3 eV or 100 kcal/mol has been found to be consistent with thresholds for proton transfer in small gas-phase clusters (Knochenmuss & Leutwyler, 1988), far less than the nonsolvated value noted above. From such considerations, it is clear that, in the highly polar condensed-phase MALDI sample (possibly also including residual hydrogen bonded solvent), it is very difficult to predict the exact energy cost of ion generation. This cost is, however, certainly several eV less than in the gas phase. This is the reason MALDI ions are observed at laser fluences that are low enough to avoid extensive fragmentation. MALDI ionization, as well as desorption, is, therefore, a *collective* phenomenon (Spengler et al., 1987; Ens et al., 1991).

Similar considerations regarding screening and ion separation in the condensed phase apply to the generation of alkali ions. In addition, it is necessary to consider the energetics of surface sites or defects in crystals. Isolated NaCl on an otherwise perfect NaCl (100) surface is much less strongly bound than in the bulk crystal; the Madelung constant in this case is only 0.066 (Hellwege, 1988)! The nominal cost of isolating these ions is only 0.3 eV or 6.8 kcal/mol. This value is again an extreme estimate, because surrounding solvent or matrix molecules will strongly stabilize the exposed surface ions; however, it shows that free alkali ions can be easily created from defect sites. No prior analyte or matrix salt formation is required.

Although ion separation in the condensed phase is not so energetically difficult as might first be feared, the final observed MALDI ions are in the vacuum. The energy required to reach this final state is given not by the condensed-phase charge separation energy, but by the gas-phase calculations with which we began. Because MALDI is a "soft" method, the condensed vs gas-phase energy difference must be made up in some process other than high-order multiphoton excitation. The most obvious source for the remaining energy is the physical expansion of the plume. Ions separated at low-energy cost in the high-density period can be pushed apart by jostling from the neutrals that are behind them, until they are too far apart to recombine in the collisionless region. In the hot unexpanded material immediately after the laser pulse, mean speeds of about 1000 m/s are likely (Beavis & Chait, 1991; Huth–Fehre & Becker, 1991; Pan & Cotter, 1992). At this speed, the energy of two collisions (1.5 eV each) suffices to fully separate ions from an initial distance of 0.5 nm. Note that forces on the ions due to typical acceleration fields of $\approx 10^6$ V/m are 10^4 weaker than the Coulomb forces, and, thus, not significant here. However, most collisions are presumably inefficient in separating ions, due to unfavorable impact angles. Therefore, charge recombination during expansion is probably extensive, as in fast atom bombardment (Sunner et al., 1986), but collisions clearly are energetically capable of finishing charge separation that has begun by another process. We now turn to those initial processes.

2. *Multiphoton Ionization*

By far, the most straightforward explanation for ions resulting from laser excitation of an absorbing organic material is single molecule multiphoton ionization (MPI), leading to a matrix radical cation:

$$\mathrm{M} \xrightarrow{n(h\nu)} \mathrm{M}^{+\bullet} + \mathrm{e}^-$$

This process has long been considered by many authors as a strong candidate for the UV MALDI primary ionization step. For example, Ehring, Karas, and Hillenkamp (Ehring et al., 1992) proposed that photoionized matrix radicals are the key to most other MALDI ions, as seen in the Fig. 3. Two of the four routes to protonated analyte proposed by Liao and Allison (Liao & Allison, 1995) also involve direct photoionization. Matrix radical cations are commonly observed for many MALDI matrices (Ehring et al., 1992), and electrons are emitted from the sample as well (Quist et al., 1994). These observations are all consistent with simple photoionization.

From its wavelength dependence (Karas et al., 1985; Heise & Yeung, 1995), it is clear that UV MALDI functions efficiently only when the laser directly excites matrix molecules. This excited state lives for a short time, some nanoseconds, and one or more further photons could be absorbed to yield the matrix radical cation and a free electron.

$$\mathrm{M} \xrightarrow{h\nu} \mathrm{M}^* \xrightarrow{m(h\nu)} \mathrm{M}^{+\bullet} + \mathrm{e}^-$$

A two-photon second step (m = 2, 3 photons overall) is unlikely, because typical MALDI irradiances of $10^6 - 10^7$

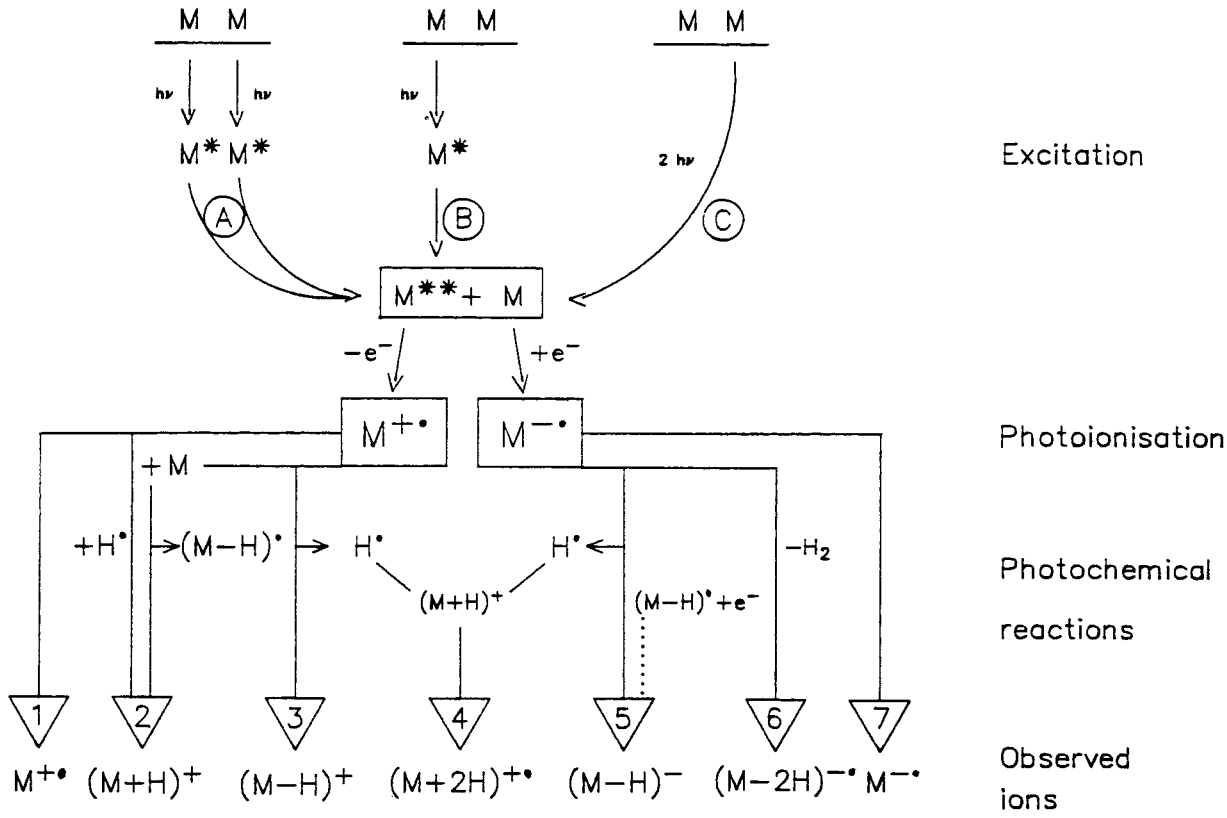

FIGURE 3. Schematic diagram of photoionization and subsequent reaction pathways in MALDI-MS, as proposed by Ehring, Karas, and Hillenkamp in 1992. Photoexcitation routes A (energy pooling), B (sequential two-photon excitation), and C (simultaneous two-photon excitation) all lead to a highly excited intermediate, which was proposed to emit an electron in the fundamental ionization step. (Copyright John Wiley & Sons, Ltd. Reproduced with permission from Ehring et al., 1992).

W/cm^2 are too low for such processes. In the simplest process (m = 1), a total of two laser photons must excite the matrix molecule from the ground state to above its ionization potential.

Ionization potentials (IPs) for matrix molecules in solid crystals or large matrix aggregates are still not known. Estimates of IPs for isolated molecules have been obtained from calculations. At the semi-empirical level (PM3 basis set) these values usually lie between 9 and 10 eV (Karbach & Knochenmuss, 1998). This range is too high for two nitrogen laser photons (7.36 eV, 169 kcal/mol); however, the accuracy of calculations is always open to question. Recently, measurements of matrix IPs have begun to appear. Using molecular beam techniques and two-color two-photon laser spectroscopy, the IP of a common matrix, 2,5-dihydroxy benzoic acid (DHB), has been determined to be 8.05 eV or 185 kcal/mol (Karbach & Knochenmuss, 1998). The photoionization efficiency curve vs total two-photon energy is shown in Fig. 4.

This IP is still higher than the energy reached by two nitrogen laser photons, but much less than the calculated value of 9.04 eV. The IP of the DHB dimer is 7.93 eV or 182 kcal/mol, not much less than that of the free molecule. Because increments per molecule in larger clusters will be much smaller, direct two-photon ionization may be still not be possible in the crystal. A larger increment has been observed for the DHB-water 1:1 cluster, where the IP is 7.78 eV or 179 kcal/mol, suggesting that DHB adjacent to analyte or crystal water may be more easily ionized than in the bulk.

In addition to DHB, the IP of 5-methoxy-2-hydroxybenzoic acid (the additive in so-called "super" DHB) has been determined by two-photon ionization, and is 7.84 eV or 180 kcal/mol. Once again, direct two-photon ionization with a nitrogen laser is not possible. Nicotinic acid is used as a matrix with 266 nm (107.2 kcal/mol or 4.66 eV) excitation from a quadrupled Nd:YAG laser. Its IP is known from photoelectron spectroscopy to be 9.38 eV, slightly above the two-photon energy of 9.32 eV (Dougherty et al., 1978). A combined photo/thermal ionization would appear to be very feasible for this molecule (see below).

MALDI irradiances are not expected to give significant 3-photon ionization yields, although little data exist regarding this possibility. Three-photon UV ionization of free DHB in the gas phase was, however, attempted and found to be

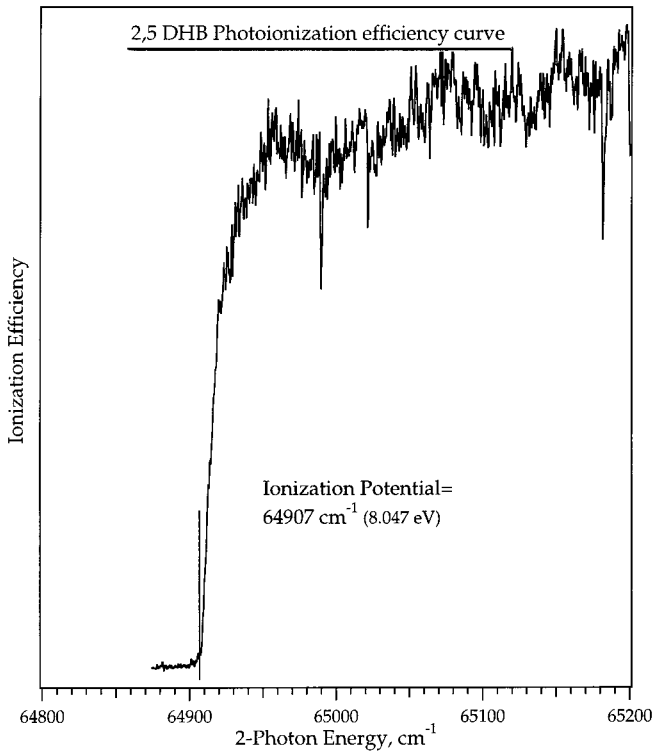

FIGURE 4. Photoionization threshold of the lowest energy rotamer of 2,5-DHB. The threshold is about 1 eV lower than all calculations, too low for electron transfer reactions with most MALDI analytes. (Adapted from Karbach & Knochenmuss, 1998.)

very inefficient, even at irradiances of up to 10^8 W/cm^2 (Karbach & Knochenmuss, 1998).

Evidence is now mounting that direct UV matrix ionization is not a common ionization mechanism, because IPs are too high. Two-photon excitation of single matrix molecules may still be part of an ionization pathway: Allwood, Dyer, and Dreyfus (Allwood et al., 1997) noted that the MALDI plume is rather hot, and thermal energy may be able to make up the difference between a two-photon excitation and the ionization potentlal. This process can be significant only if the IP is not far above the two-photon energy, as seems to be the case for some matrix molecules. This combined photo/thermal mechanism will be discussed further in conjunction with energy pooling below.

Whereas most MALDI experiments are still performed with UV lasers, IR excitation has recently become more widespread. At 2.94 μm, for example, the photon energy is only 0.43 eV or 9.8 kcal/mol, and many photons would be required to reach the matrix IP. On the other hand, IR MALDI fluences are higher than for UV MALDI by 1–2 orders of magnitude, and the ion yield per desorbed neutral is orders of magnitude lower. A (very inefficient) multiphoton ladder-climbing excitation/ionization process is, therefore, conceivable.

3. Energy Pooling and Multicenter Models

Whether or not direct multiphoton ionization is possible, excited states of matrix molecules play an important role in UV MALDI (Preston–Schaffter et al., 1994; Ehring & Sundqvist, 1995; 1996; Ehring et al., 1996). One possibility is excited-state proton transfer from matrix to analyte, which will be discussed in Section III.A.4. Another possibility is that two or more separately excited matrix molecules pool their energy to yield one matrix radical cation or a highly excited matrix molecule. Such a mechanism is attractive, because it explains how energetic processes can occur in a diffusely excited solid. It is plausible, because strong interactions between closely packed chromophores in solids are common, and because clusters are known to be produced in MALDI plumes (Cramer et al., 1997; Puretzky & Geohegan, 1997; Zhigilei et al., 1997; Handschuh et al., 1998). A number of authors have included this model in the range of possibilities, as in Fig. 3 (Karas et al., 1993; 1996; Johnson, 1994; Ehring & Sundqvist, 1995; 1996; Knochenmuss et al., 1996).

$$\mathrm{MM} \xrightarrow{2h\nu} \mathrm{M^*M^*} \rightarrow \mathrm{M} + \mathrm{M^{+\bullet}} + \mathrm{e^-} \text{ (or other matrix ions)}$$

$$\mathrm{M^*M^*} + \mathrm{A} \rightarrow \mathrm{MM} + \mathrm{A^{+\bullet}} + \mathrm{e^-} \text{ (or other analyte ions).}$$

There are several indications that more than one excited matrix molecule is needed to generate ions in MALDI. In an important fluorescence study of solid matrices, Ehring and Sundqvist showed that luminescence was quenched at excitation densities that correspond roughly to the MALDI threshold (Ehring &Sundqvist, 1995). This was interpreted as due to exciton annihilation (reaction of two excited molecules with each other). The fluorescence spectrum was also

TABLE 2. Ionization potentials of some MALDI matrices and matrix complexes.

Matrix	Ionization potential (eV)	Reference
2,5 DHB	8.05	Karbach & Knochenmuss, 1998
$(2,5\ \mathrm{DHB})_2$	7.93	
2,5 DHB · H_2O	7.78	
5-Me-2-OH-benzoic acid	7.84	
2,3 DHB	8.27	
nicotinic acid	9.38	Dougherty et al., 1978

IPs were measured by two-color two-photon ionization, with the exception of nicotinic acid, which was studied with photoelectron spectroscopy. Values where no reference is indicated are unpublished results from our laboratory.

broadened in a manner that suggested exciton formation. At the threshold fluence for desorption of neutral DHB, the excitation density is one molecule in 17, which corresponds to a mean distance between excitations of about 2 molecular diameters; i.e., they are nearly touching. The apparent ionization threshold lies higher, at about one excitation per 4 molecules; thus, excited pairs become quite common.

As discussed in Section II.B, MALDI signals depend on laser fluence rather than irradiance or peak power. Time-delayed two-pulse experiments (Knochenmuss et al., 1996; Tang et al., 1997) also show that, on a time scale of about 10 ns, MALDI depends on the number of photons delivered, not on the rate at which they arrive. In DHB, the optimum time delay for two-pulse excitation is near the fluorescence lifetime; thus, it is probably a singly excited matrix that acts to store energy. Arrival of a second photon can initiate ion production. For statistical reasons, at typical MALDI laser fluences, it is more likely that a neighbor of an excited matrix will be the next to become excited, rather than that the excited molecule will be hit by a second photon. An energy-pooling mechanism for ion formation will, therefore, be statistically favored, if it can occur.

The matrix suppression effect also suggests a multicenter ionization model (Knochenmuss et al., 1996): at sufficiently high analyte concentration, matrix ion signals can be completely suppressed in MALDI. This effect will occur either in the positive or negative mode, but not both (Knochenmuss et al., 1998). The effect is most straightforwardly explained if ionization is an immediate consequence of coalescence of two excitations, or exciton pooling. The product is either a matrix ion, or, when analyte is present, an analyte ion. Matrix suppression appears when all excited matrix molecules are in close proximity to analyte; proximity depends on the size and concentration of analyte in the sample. This picture was supported by the fluence dependence of suppression, a time-delayed two-pulse experiment, and by dilution with inert materials (Knochenmuss et al., 1996). The analyte size dependence of the effect was also consistent with the model (Knochenmuss et al., 1998).

Protonated analyte ions have been observed as photoionization products of laser-desorbed clusters (Krutchinsky et al., 1995; Meffert & Grotemeyer, 1995; 1998; Land & Kinsel, 1998). Land and Kinsel (Land & Kinsel, 1998) have shown that the process requires two photons, and appears to proceed via intermediate ionization of the matrix (Fig. 5). Because ions are created out of clusters in these studies, a multicenter mechanism is quite possible. Alternatively, the IP of individual matrix molecules may be lowered by clustering. The neutral cluster sizes and compositions were not known, nor was it clear whether the proton was transferred before or after ionization. An asymmetric fragmentation of the photoionized cluster seems to be the more likely mechanism (Krutchinsky et al., 1995; Land & Kinsel, 1998).

Nearest-neighbor energy-pooling ionization has been explicitly modeled in an extension of the photo/thermal model of Allwood, Dyer, and Dreyfus (Allwood et al., 1997a; 1997b). Using measured parameters for the matrix properties, Karbach and Knochenmuss (Karbach & Knochenmuss, 1998) showed that, for a DHB matrix, even very modest pooling rates, similar to or less than the decay rate of the excited state, can lead to substantial ion production, much in excess of the yield without pooling (Fig. 6). No reduction in IP due to clustering was assumed; thus, true ionization rates could be even higher, because the efficiency of the thermal step goes as the inverse exponential of the energy deficit from the doubly excited state to the ion.

4. Excited-State Proton Transfer

After photoionization, excited-state proton transfer (ESPT) is possibly the most frequently proposed MALDI ionization model, and goes back to the origins of MALDI (Karas et al., 1987). It is very attractive, because it requires only one photon. A singly excited matrix molecule is presumed to become much more acidic than when in its ground state. Nearby analyte or ground-state matrix may accept a labile proton before the excited molecule relaxes.

$$M + h\nu \rightarrow M^*$$

$$M^* + A \rightarrow (M - H)^- + AH^+$$

$$M^* + M \rightarrow (M - H)^- + MH^+$$

Such excited-state acidity enhancement has been known in solution since early studies on saliclyates and phenols. Aromatic hydroxyl or amine groups are, in many cases, excited-state acids. Jumps in pK values of 9 or more units are known (Ireland & Wyatt, 1976). Although many matrices are carboxylic acids, COOH groups are not generally affected by electronic excitation (Ireland & Wyatt, 1976). The role of aromatic hydroxyls in proton transfer to analyte is hinted at by experiments, where acid groups were esterified yet hydroxyl-containing matrices remained effective (Karas et al., 1996). Derivatization of the hydroxyl groups was found by some authors to strongly degrade MALDI efficiency (Karas et al., 1996), whereas others came to the opposite conclusion (Grigorean et al., 1996).

Excited-state proton transfer has been proposed since the time of MALDI-like laser desorption experiments (Karas et al., 1985), and taken up by various groups since then (Gimon et al., 1992; Spengler & Kaufmann, 1992; Chiarelli et al., 1993; Krause et al., 1996; Yong, 1998). However, none of the popular matrices is known to be particularly ESPT-active in solution or the gas phase, nor have established ESPT compounds generally functioned well as matrices; many of those tested are instead rather bad (Ehring et al., 1992).

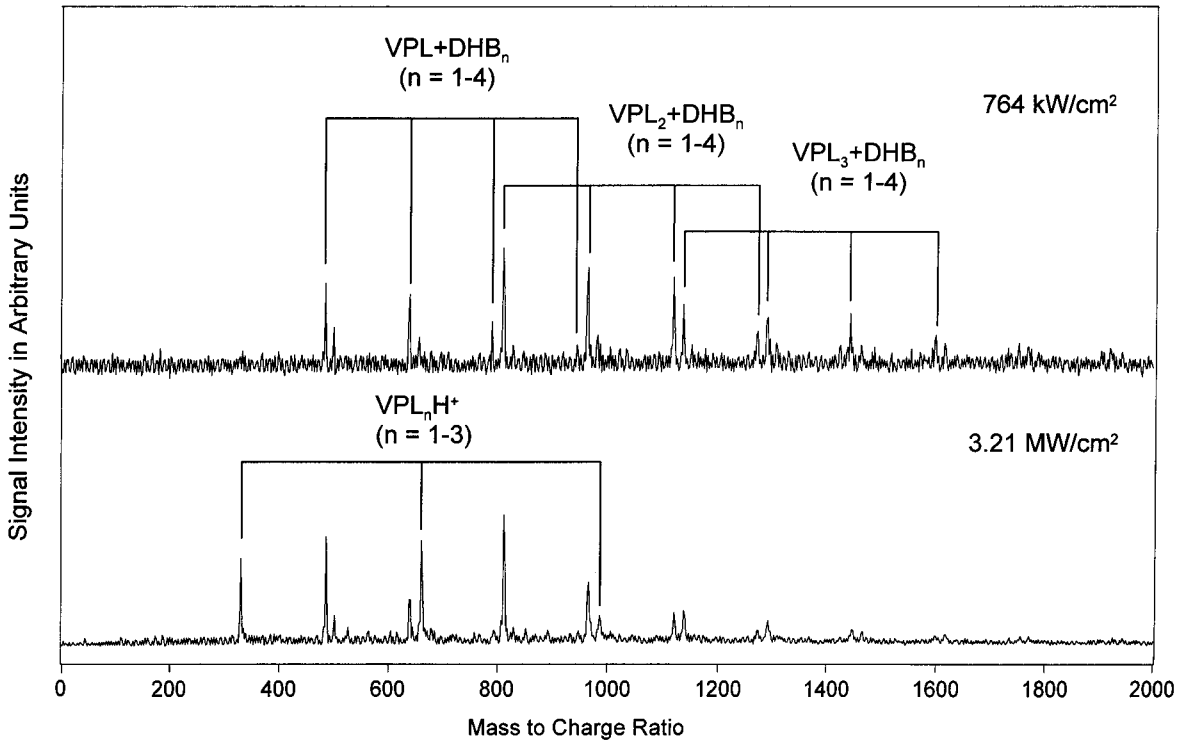

FIGURE 5. Laser power-dependent mass spectra from 308 nm photoexcitation of mixed clusters of valiyl-prolyl-leucine (VPL) and 2,5-DHB. Clusters are formed by entrainment in argon supersonic jet expansions. The two-photon energy is just below the ionization energy of DHB; thus, at low laser powers, the mixed VPL+DHB dimer radical cation represents the lowest mass product ion observed. As power is increased, mixed radical cation clusters absorb additional photons, leading to DHB to VPL intracluster proton transfer and/or asymmetric cluster dissociation to form $VPLH^+$ and $(VPL)_nH^+$ product ions (with permission from Prof. G. Kinsel, University of Texas at Arlington).

Many good UV matrices are structurally similar to ESPT species like salicylic acid, in that a hydroxyl group is ortho to a carbonyl moiety (CO, COOH, $CONH_2$). In excited salicylic acid, the hydroxyl proton is transferred to the carbonyl oxygen, as in Fig. 7.

On the assumption that the labile proton can be just as easily given to an analyte, this structural feature was used to propose a class of matrices, of which several were considered quite effective (Krause et al., 1996). Corresponding meta- and para-hydroxy isomers were evaluated as much less effective. The ESPT premise of this work remains interesting, but unproven. Only two of the molecules studied (salicylic acid and salicylamide) are known to exhibit ESPT in solution or the gas phase, and it is by no means certain that all molecules with the ortho-hydroxy carbonyl structural element are active. Indeed, the popular matrix DHB is the 5-hydroxy derivative of salicylic acid, and might thus be expected to be a classical ESPT molecule. However, it has been shown by fluorescence in solution, gas phase, and clusters that this is not the case (Karbach & Knochenmuss, 1998). The electron-withdrawing effect of the second hydroxyl group inhibits ESPT. The closely related 5-methoxy-2-hydroxy benzoic acid ("super" DHB additive) is also not ESPT-active (Karbach & Knochenmuss, 1998).

Exchange of Li^+ ions for protons in similar molecules as well as in carboxylic acid derivatives of fluorene was taken as evidence for ESPT in a MALDI experiment (Chiarelli et al., 1993). Up to three lithium ions were attached, with the loss of two protons for a net charge of one. These unusual ions resemble those formed in other systems, where no ESPT has been proposed, as mentioned in Section III.B.5. 3HPA is an effective matrix for studying DNA, and contains the ortho-hydroxy carbonyl unit. Some evidence exists that it undergoes an intermolecular ESPT reaction in hydrogen bonding solvents; that process was inferred to contribute to its efficacy as a matrix (Wu et al., 1994).

The possible ESPT reactivity of aromatic amines in MALDI has been the object of some study (Gimon et al., 1992; Gimon–Kinsel et al., 1997). The MALDI efficacy of para-substituted anilines was correlated with calculated properties of the corresponding protonated species (anilinium ions). The source of the anilinium ions remains uncertain, and the reaction may not involve excited states.

Some popular and effective matrices are cinnamic acid

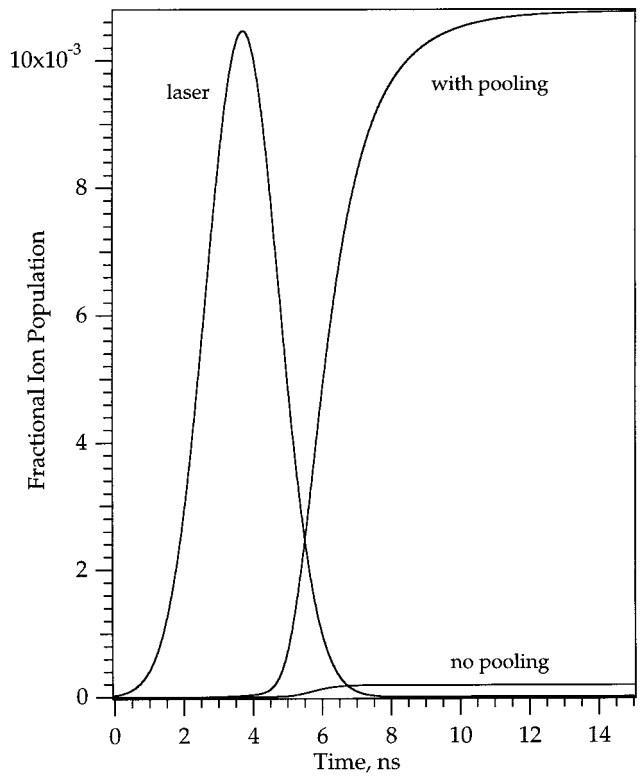

FIGURE 6. Photo/thermal ionization model with and without the two-center energy-pooling process described in the text. In both cases, measured parameters for DHB are used. The laser pulse is shown scaled to fit the graph. Constants specific to DHB were: ionization potential = 8.05 eV, energy of first excited state = 3.466 eV, excess energy in S_1 after 377 nm excitation = 0.21 eV, energy gap from upper excited state to ion = 0.90 eV, S_1 lifetime = 5 ns, solid state quantum efficiency = 0.2. (Copyright John Wiley & Sons, Ltd. Reproduced with permission from Karbach & Knochenmuss, 1998).

derivatives, which do not have ortho-hydroxy carbonyl features, although a phenolic hydroxyl group is present. An ESPT mechanism for such materials has been proposed on the indirect basis of three-photon fragmentation patterns of ammonia, methyl amine, and ammonia/methanol clusters (Yong, 1998).

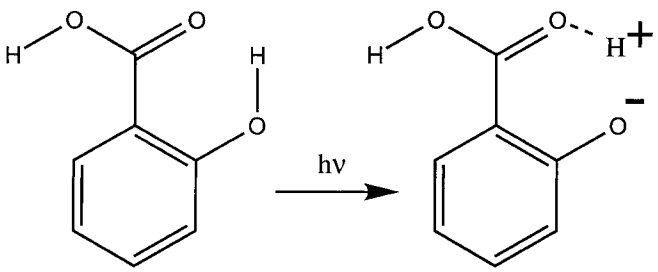

FIGURE 7. Intramolecular excited-state proton transfer in salicylic acid. The ortho-hydroxy carbonyl structural unit is a common feature of many MALDI matrices, and has been proposed to improve ion yields by proton transfer to the analyte (Krause et al., 1996).

A route to enhanced MALDI signal, which does not appear to have been widely pursued, is enhanced photobasicity of the analyte, perhaps via derivatization. A possible example of such reactions is provided by the triple protonation of spirooxazines in sinapinic acid matrix (Calba et al., 1997). These materials undergo a photolytic ring opening, which seems to be associated with abstraction of three protons from the matrix. Excited states of aromatic side groups were also proposed to enhance protonation of some peptides (Olumee et al., 1995).

A factor that is widely neglected in the discussion of ESPT in MALDI is that EPST in solution is highly sensitive to the solvent environment. From the discussion above regarding energetics of ion separation, the reason for this sensitivity is clear. Without intra- or intermolecular assistance, ESPT is too costly for a single near-UV photon. The near-complete lack of knowledge regarding the local environment in a MALDI sample is a major limitation in evaluating or implementing this mechanism.

5. Disproportionation Reactions

One of the notable facts of MALDI is that a given matrix will often perform in positive and negative ion modes. Positive and negative matrix signals can give the qualitative impression of being correlated: M^+ with M^-, or MH^+ with $(M-H)^-$. This correlation suggests that disproportionation reactions may be an active ionization mechanism:

$$2M \xrightarrow{nh\nu} (MM)^* \rightarrow (M - H)^- + MH^+$$

$$\text{and/or} \rightarrow M^- + M^+$$

In view of the evidence for a multicenter process, it is possible to describe these reactions as an excitation of a strongly coupled matrix pair. This possibility is important, because a two-step process (ESPT or photoionization followed by capture of a proton or electron) will be limited by the activation energy of the first step. A concerted process can have a much lower activation energy for the same net thermodynamics.

Little is currently known about this possibility, but the energetics are interesting. Recent measurements have yielded the gas-phase basicities of some matrix neutrals (see Table 4, later in this article) and anions (Table 5, later in this article) (Taft & Topsom, 1987; Breuker et al., 1998). From these data, the free energy changes for the proton disproportionation reaction are immediately available (Table 3).

Assuming a reasonable activation energy and a concerted mechanism, these reactions are easily initiated by two nitrogen laser photons. Nonconcerted two-step reactions are

TABLE 3. Energy requirements for disproportionation reactions $2M \rightarrow (M - H)^- + MH^+$ (Breuker et al., 1998).

Matrix	kcal/mol	eV
DHB	121	5.24
3HPA	120	5.18
NA	118	5.10
THA	113	4.89

DHB = 2,5 dihydroxybenzoic acid, 3HPA = 3-hydroxypicolinic acid, NA = nicotinic acid, THA = 2,4,6-trihydroxyacetophenone

not energetically possible. For example, the energy needed to eject a proton from DHB (i.e., the basicity of the DHB-H anion) is 317 kcal/mol or 13.8 eV; other matrices lie even higher (Breuker et al., 1998).

Energy requirements for electron disproportionation reactions are more difficult to estimate, because the required electron affinities (EA) are not known. However, for single ring aromatics with electron-withdrawing groups, EAs are typically about 1.1 eV (unsubstituted benzene has a negative electron affinity) (Harrison, 1992). The IPs of DHB and NA are 8.05 and 9.38 eV, respectively, for a net reaction energy of 7–8.3 eV or 160–190 kcal/mol, respectively. This value is not a great deal less than for direct photoionization, but *is* accessible with two of the appropriate laser photons (nitrogen or Nd:YAG 3rd harmonic).

Although a concerted disproportionation mechanism can bring the instantaneous energy requirements down to within a two-photon range, the evidence for it is not yet strong. Positive and negative matrix ions are not necessarily correlated in the manner required, and thresholds are sometimes different for the two polarities.

6. *Desorption of Preformed Ions*

One attractive mechanism is that the ions observed in the MALDI mass spectrum are already present in the solid sample and are merely liberated by the laser pulse. This mechanism is potentially most relevant for compounds that are intrinsically ionic in character, such as the "tagged" materials discussed below, or molecules that form strong (and possibly specific) metal– ion complexes, such as crown ethers, ionophores, or metal-binding proteins (Lehmann, 1996). For preformed complex ions, if the appropriate metal is present at sufficiently high concentration in the sample, the corresponding metal adduct is generally detected, rather than the protonated species.

If the analyte is ionic in nature to begin with, then the thermodynamics of this process are similar to that of liberation of salt ions. As noted above, the larger the ions, the easier the separation; thus, this process may be relatively easy for many organic ions. If the preformed ion is a complex of neutral analyte with a cation from added salts, then the energy requirements may also be moderate if the ion is fully enclosed by the analyte (rather than on its surface), leading to a large effective radius for the ionic complex.

Preformed complex ions prepared in solution must be mixed with matrix before analysis, and the matrix may compete with the analyte for ions. For example, complexation constants of deprotonated DHB with transition metal ions were found to be rather high, whereas those constants with polystyrene were estimated to be much lower (Lehmann et al., 1997). A preformed ion that is stable in solution may break apart thermally in the gas phase, if it is too weakly bound in the absence of solvation effects. Lithium ion affinities for simple oxygen- or nitrogen-containing molecules are in the range of 35–45 kcal/mol (1.5– 2 eV) (Klassen et al., 1996; Rodgers & Armentrout, 1997). Affinities for the larger sodium cation are less, near 30 kcal/mol (Guo et al., 1989; Klassen et al., 1996). Large monovalent ions will be the least well bound, and multivalent ions will be more effective cationizing agents due to greater electrostatic forces. Larger analytes with multiple polar sites available for coordination may have particularly high gas-phase cation affinities, as was shown for sodiated polyethylene glycol oligomers (von Helden et al., 1995).

Allison and co-workers (Liao & Allison, 1995) have presented a method that apparently relies on preformed ions. The peptide analytes are "charge tagged" by covalently attaching a phosphonium group to either terminus, dramatically enhancing detection sensitivity. Ehring et al. (Ehring et al., 1996) presented an interesting study that compared front-side and back-side laser illumination of samples deposited on a 200-nm gold film. With back-side illumination, no photochemistry is possible, yet small peptides (e.g., gramicidin S) were observed, exclusively in the form of cationized species. This finding was interpreted as thermal desorption of preformed ions. Zhu et al. (Zhu et al., 1995) found very different detection efficiencies for peptides with and without basic amino acid residues. They argued that proton transfer in solution governs the detection efficiency, and that this "preprotonation" mechanism lowers the barrier for ionization of peptides in MALDI. Their results do not, however, exclude gas-phase protonation.

It is difficult to be certain that ions observed in the mass spectrum are truly preformed and are not the result of secondary gas-phase chemistry in the plume. Cationization of some copper- and zinc-binding peptides is most easily explained by desorption of the covalent complex species, rather than by gas-phase cationization (Nelson & Hutchens, 1992; Woods et al., 1995; Lehmann et al., 1998; Masselon et al., 1998). For example, Lehmann et al. (Lehmann et al., 1997) have used IR, visible, and NMR spectroscopy to investigate the degree of preformed metal-complex ions in MALDI samples, and correlated this degree with MALDI spectra. Clear indications for preformed ions were found for these

systems. It was shown that their contribution to the MALDI spectrum could be predicted on the basis of condensed-phase association constants.

Preformed negative ions may be important for some ionic analyte classes, particularly when using matrices that are basic in solution (Fitzgerald et al., 1993). Oligonucleotides may sometimes fall into this class, but little or no work has been done to establish the extent of preformed or gas-phase ion generation. Molecules with sulfonate functionalities are sometimes observed as preformed ions, particularly in the form of electrostatically bound complexes (Juhasz & Biemann, 1994; Salih & Zenobi, 1998). Preformed negative ions might be expected in MALDI, by analogy to metal ion complexes in positive mode. These ions are apparently quite rare, if they exist at all. The anions can, in principle, be neutralized by matrix cations, or can react by proton transfer to form neutral molecules such as HCl from Cl^-. However, it is not clear why such processes should be so efficient, when neutralization reactions of matrix and analyte are not.

7. *Thermal Ionization*

In two-phase MALDI, the liquid containing the analyte is generally transparent to the incident laser, which may be of any wavelength that is absorbed by the particles. Because black materials such as graphite, silicon, or TiN are typically used, any visible or near UV laser is suitable. Because the liquid is not directly excited, it is very probable that desorption and ionization take place via thermal mechanisms. Time-resolved infrared emission experiments in our laboratory have shown that a typical two-phase 2-μm graphite/glycerol sample reaches peak temperatures of 700–900 K in a few nanoseconds when irradiated with a nitrogen laser under typical MALDI conditions. Smaller particles work better for MALDI, and were found to reach higher peak temperatures. The cooling is less rapid, on a time scale of 100 ns.

Thermal ionization in a two-phase experiment can take place in two ways: directly at the particle surface, or in the bulk of the liquid matrix. In the first case, and assuming thermal equilibrium between all degrees of freedom, the extent of ionization of species I, α_i, will be given by the Saha–Langmuir equation (Fujii, 1996):

$$\alpha_i = C \exp((\phi - IP_i)/kT),$$

where C is a constant near unity, and ϕ is the work function (ionization potential) of the particle surface. The IPs of aliphatic alcohols like glycerol are above 10 eV, and the work function of graphite is near 5 eV; thus, α is negligible ($\approx 10^{-25}$) at 1000 K. Two factors probably contribute to the observed efficacy of two-phase MALDI. First, the smaller the particle, the higher the peak temperature. The sample-averaged measured temperatures of about 1000 K do not reflect the role of very fine particles. Schürenberg has estimated that peak temperatures of 35-nm particles are above 10,000 K (Schürenberg, 1996). This temperature gives $\alpha_i =$ of 3×10^{-3} on graphite, which is comparable to normal UV MALDI. Second, a higher surface work function rapidly increases the efficiency of the process. Partially oxidized metal surfaces are routinely used in surface ionization mass spectrometry for this reason (Fujii, 1996). Oxidized sites or regions on a particle could serve the same function, and the high work function of nitrides may be the reason why TiN is a particularly good two-phase particulate material. Even at 5000 K, a work function of 7 eV gives an ion yield of 10^{-3}. Addition of aromatic compounds in small quantities has been found in our laboratory to improve two-phase ion signals; this improvement may be a result of the much lower IPs (e.g., 8.05 eV for DHB).

Thermal ionization may, in principle, also occur in the matrix bulk. The reaction is effectively disproportionation, and the extent can be described by an equation of the same form as for surface ionization; however, the work function is replaced by the electron affinity of the matrix:

$$2\mathrm{M} \xrightarrow{\Delta H} \mathrm{M}^- + \mathrm{M}^+ \quad \alpha_i = C \exp((EA - IP_i)/kT).$$

Electron affinities of matrix molecules are expected to be quite low, near 1 eV, as discussed above. Thermal ionization in MALDI by this route, therefore, requires very high temperatures.

Mowry and Johnston have found that the internal energy of molecules desorbed in normal UV MALDI corresponds to effective temperatures of around 500 K (Mowry & Johnston, 1994). A thermal ionization/disproportionation reaction at these temperatures is clearly not significant. In laser desorption experiments without matrix, irradiances of 10^6 W/cm^2 (but high pulse energies of up to 500 mJ) have been reported to yield temperatures of up to 3000 K, and K^+ ion emission was described as kinetically rather than thermally limited, with an activation energy of only 0.6 eV or 14 kcal/mol (Cotter, 1987). Bulk thermal ionization in UV MALDI may, thus, play some role, but it is unlikely to be dominant. Thermal proton disproportionation is energetically more favorable (see Section III.A.5) and may make some contribution.

It should be noted here that the "quasi-thermal" model of the Hillenkamp group for MALDI ion production describes the empirical rate of ion emission from the solid sample without implying a thermal mechanism for the microscopic ionization step (Dreisewerd et al., 1995). As such, the model adds to our understanding of desorption, but not of primary ion formation. Indeed, at their derived peak temperatures of less than 500 K, little direct thermal ionization is to

be expected. What their model clearly shows is that ions are not released from the sample without concomittant neutral desorption. This model is consistent with the arguments above regarding final ion separation by collisions.

8. Pressure Pulses, Spallation, and Shocks

The MALDI laser pulse physically damages the crystalline sample on a time scale of a few nanoseconds. Because of the high absorption coefficient, in UV MALDI this damage is limited to a region of up to a micrometer in thickness. In IR MALDI, the laser penetrates much deeper, so the sample might be removed down to the substrate. It has been proposed that this rapid mechanical stress results in desorption of ions in a manner reminiscent of fast atom bombardment or secondary ion mass spectrometry (Lindner & Seydel, 1989). Certainly the phenomenon of triboluminescence shows that electronic excitation can result from crystal breakage. A related pressure-pulse model has been developed primarily by Johnson (Johnson & Sunqvist, 1991; Johnson, 1994; 1996). In this model, the ions may actually be formed in a two-center excitation annihilation event as discussed above, and rapidly ejected by the sudden destruction of the solid.

Due to the weakness of IR absorptions, the energy per volume deposited in an IR MALDI experiment is quite low on average, too low even to fully melt the material that is desorbed. Taking this factor into account, Cramer, Haglund, and Hillenkamp have proposed that spallation is an important mechanism in IR MALDI (Cramer et al., 1997). Thermally induced stress that builds faster than can be dissipated by emission of acoustic waves leads to a mechanical failure of the solid and an ablation of material without direct vaporization. This step is accompanied by ion and electron emission, presumably due to stress-induced electric polarization of the separating solid surfaces (piezoelectricity). The strength of the argument for this mechanism has been reduced, because it has been recognized that, in UV and IR MALDI, deposited energy densities *at the surface of the sample* are about the same (1 eV/molecule) (Chen et al., 1998).

Laser-induced shock waves are routinely used in laboratory research of high-pressure phenomena, but apparently rather little is known about shocks in molecular solids. Recent studies of laser-induced shocks in solid anthracene found pressures of > 4 GPa, front speeds of 4 km/s, and a front width of 100 molecules (Dlott et al., 1998). The temperature jump measured with coherent anti-Stokes Raman scattering was rather modest, with a peak of about 650 K. This value suggests very limited ion production via thermal mechanisms in shocked MALDI samples.

B. Secondary Ionization Reactions in the MALDI Plume

Plausible secondary ionization mechanisms must take into account the conditions existing in the MALDI plume, which we summarize first. Reaction pathways leading to observed analyte ions may be simple or may entail multiple steps. Matrix–matrix reactions may be necessary to provide intermediates, which ionize analyte. The most important secondary reactions are those leading to protonated and cationized analyte. Particularly for the former, sufficient data are now available to allow thermodynamic analysis of the possible pathways.

1. MALDI Plume

Molecular dynamics simulations show that the UV MALDI plume can be described as a very rapid, even explosive, solid-to-gas phase transition (Vertes et al., 1993; Zhigilei et al., 1997; Zhigilei & Garrison, 1998). With nanosecond laser pulses, the time required for significant expansion is tens of nanoseconds (Vertes et al., 1993). Densities are still several percent of the solid density for up to 100 ns after the laser pulse. Even at 6 ms after the laser pulse, and 3 mm above a HPA sample, Puretzky and Geohegan measured a neutral molecule density of about 10^{-4} atmospheres, implying a rather high residual collision rate (Puretzky & Geohegan, 1997).

In addition to single molecules, clusters or aggregates of matrix are also ejected, particularly in IR MALDI (Cramer et al., 1997; Puretzky & Geohegan, 1997; Zhigilei et al., 1997; Handschuh et al., 1998). Optimization of the laser fluence can probably minimize the amount of clusters produced, as implied in the work of Garrison and co-workers (Zhigilei & Garrison, 1997; Zhigilei et al., 1997). The fraction of free molecules and small clusters is greatest at low laser fluences, close to threshold for ion production; however, the absolute ion yield may be greater at elevated laser irradiance. As noted in Section III.A.8, IR MALDI desorption may involve much less direct vaporization than UV MALDI, and may be more mechanical in nature.

Although desorption continues for a considerable time after the laser pulse (Quist et al., 1994), the observed ions appear to be generated very quickly (Puretzky & Geohegan, 1997). Post-plume matrix ion velocities on the axis reach up to 1000 m/s, and vary between matrices (Beavis & Chait, 1991; Huth–Fehre & Becker, 1991; Pan & Cotter, 1992; Spengler & Bökelmann, 1993; Juhasz et al., 1997). Analyte ions are 100–200 m/s slower in general (Zhou et al., 1992; Juhasz et al., 1997), and there are fast and slow components (Kinsel et al., 1997). The slow component exhibits an energy deficit vs the nominal acceleration voltage, presumably due to numerous collisions (Zhou et al., 1992). The plume develops a directionality toward the laser beam, and the emit-

ted ions have a roughly cosine intensity distribution about this axis (Westman et al., 1994; Aksouh et al., 1995).

After the initial temperature jump, some jet expansion cooling is predicted, but internal energies downstream are found to remain rather high, about 500 K (Mowry & Johnston, 1994; Dreisewerd et al., 1995), possibly because large polyatomic molecules do not cool efficiently. Small fragment molecules may help cool more effectively, such as H_2O or CO_2 formed by thermal decomposition.

From these studies, the current view of the plume is that primary ions are created in a moderately hot, dense bath of neutral matrix molecules and clusters, and many will undergo collisions before being extracted into the drift region of the mass spectrometer. Secondary ion–molecule reactions are to be expected. The final ions observed in the MALDI mass spectra can, in principle, be completely different from the primary ions. Of particular importance are proton-transfer reactions, cationization reactions, and electron-transfer reactions.

2. *Gas-Phase Proton Transfer*

a. Matrix–matrix reactions. Matrix–matrix reactions certainly occur in the plume, and some may be essential for providing intermediates that can protonate analytes (Ehring et al., 1992). If primary ions are radical cations, hydrogen atom transfer, or (more likely) proton transfer, can lead with high efficiency to protonated matrix (Harrison, 1992):

$$M^{+\bullet} + M \rightarrow MH^+ + (M - H)^{\bullet}$$

The resulting radical $(M\text{-}H)^{\bullet}$ may capture a free electron to form the even-electron $(M\text{-}H)^-$. This reaction is believed to be the main route for formation of protonated glycerol in fast atom bombardment (FAB) mass spectrometry (Sunner, 1993). In the case of matrices with phenolic OH groups, decay of the protonated species gives $(M\text{-}OH)^+$ and H_2O as products. This fragmentation route is sometimes observed in MALDI mass spectra, but is not always found after simple photoionization of free matrix molecules.

Protons are particularly mobile in hydrogen-bonded networks such as water. In matrix clusters, they are certainly much less mobile, but possibly mobile enough to migrate some distance until trapped by an analyte with higher proton affinity.

The matrix may also undergo a dissociative electron-capture reaction similar to that proposed for FAB (Sunner, 1993):

$$M + e^- \rightarrow (M - H)^- + H^{\bullet}$$

The hydrogen atom is presumably lost from a hydroxyl group, leaving an oxygen-centered anion. Evidence for this mechanism exists in the fact that H atoms have been found in significant quantities in MALDI plumes (Scott et al., 1994).

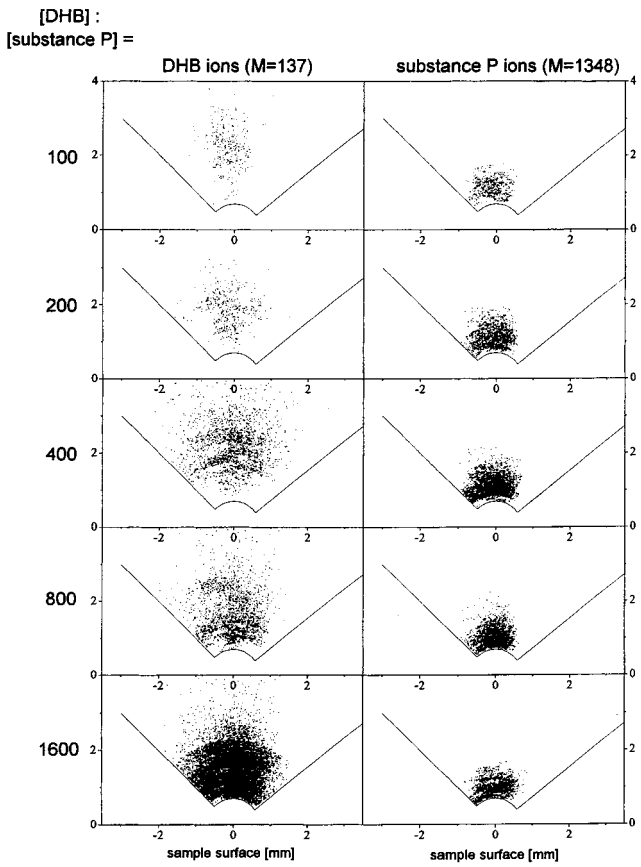

FIGURE 8. Ion density plots of matrix and analyte ions obtained at various molar ratios of matrix to analyte (dried-droplet method). Angle of incidence of the laser beam was −60° with respect to the surface normal. The straight line marks the measured angle. (Reprinted by permission of I.M. Publications from Bökelmann et al., 1995. Copyright I.M. Publications 1995.)

b. Matrix-analyte reactions. As pointed out by Ehring et al. (Ehring et al., 1992), secondary proton-transfer reactions are obviously important in MALDI, because many molecules appear in protonated form in the mass spectra. In one of the more important experimental demonstrations of this phenomenon, Bökelmann et al. (Bökelmann et al., 1995) investigated ion angular and velocity distributions in a MALDI plume, and found a depletion of matrix ions in areas of high AH^+ analyte ion density. The presence of protonated analyte also eliminated a slow matrix ion component of the same velocity as the analyte. These data were interpreted as evidence for either ion–molecule or ESPT reactions in the plume. (See Fig. 8.)

Photodissociation (Preisler & Yeung, 1997) and flight time studies (Kinsel et al., 1997) of protonated MALDI analytes have also given strong indications of secondary proton transfer plume reactions.

TABLE 4. Proton affinities and gas-phase basicities of MALDI matrices and selected model analytes (amino acids, peptides).

Compound	Measured proton affinities (kcal/mol)	Measured gas-phase basicities (kcal/mol)	References
Ferulic acid	210* Ave: 196.5		Jørgensen et al., 1998
	183		Burton et al., 1997
4HCCA	223 Ave: 202.5	215	Steenvoorden et al., 1997
	183		Burton et al., 1997
	201*		Jørgensen et al., 1998
	203**		Nelson et al., 1996
2,5-DHB	204 Ave: 204		Burton et al., 1997
	202.9		Nelson et al., 1996
	204	197	Steenvoorden et al., 1997
HABA	225* Ave: 204		Jørgensen et al., 1998
	183		Burton et al., 1997
Caffeic Acid	207*		Jørgensen et al., 1998
Dithranol	209		Burton et al., 1997
Sinapinic acid	214 Ave: 210	206	Steenvoorden et al., 1997
	204		Burton et al., 1997
	212*		Jørgensen et al., 1998
	210		Nelson et al., 1996
2,4,6-Trihydroxyacetophenone	210.8		Nelson et al., 1996
3-hydroxypicolinic acid (HPA)	214* Ave: 214		Jørgensen et al., 1998
	214.5		Nelson et al., 1996
trans-3-indoleacrylic acid	215		Burton et al., 1997
Nicotinic acid	217* Ave: 216		Jørgensen et al., 1998
	215		Burton et al., 1997
Picolinic acid	217*		Jørgensen et al., 1998
Glycine	210.5	202.7	Harrison, 1997
Lysine	235.6	221.8	Harrison, 1997
Arginine	244.8 (247.8*)	237.0	Harrison, 1997
Gly_7		230.2	Wu & Fenselau, 1992
GlyHis		225.3 (227.8*)	Carr & Cassidy, 1996
GlyGlyArg		242.6	Wu & Fenselau, 1993

Method of determination: bracketing. Kinetic method used where marked with *.
** Calculated value.

When the proton-transfer reaction

$$MH^+ + A \rightarrow M + AH^+$$

has a $\Delta G < 0$, it is generally very efficient in the gas phase (Harrison, 1992). Often, ΔG values are not available, so ΔH values (proton affinities or PA) are used instead. Note that, in a hot plume, neglect of entropic effects may give rise to some errors. Proton affinities of peptides and proteins are on the order of 240 kcal/mol (Harrison, 1997). Proton affinities of MALDI matrices have only begun to be measured. All currently known values are summarized in Table 4.

Measured values vary between 183–225 kcal/mol. Therefore, proton transfer to a neutral gas-phase peptide or protein will almost always be thermodynamically favorable. Sensitivity will also be improved, if the protein or peptide contains a basic residue (Zhu et al., 1995) and maybe with increasing chain length (Olumee & Vertes, 1998). Proton transfer will be favorable for most nitrogen-containing or-

TABLE 5. Gas-phase basicities of deprotonated matrix species (adapted from Breuker et al., 1998).

$(M - H)^-$ derived from	GB($(M - H)^-$) (kcal/mol)
3-aminoquinoline	347 ± 2.7
para-nitroaniline	337 ± 2.7
	336 ± 2*
2-amino-5-nitropyridine	334 ± 2.7
2-amino-3-hydroxypyridine	334 ± 2.7
nicotinic acid	326 ± 2.7
3-hydroxypicolinic acid	326 ± 2.7
2,5-dihydroxybenzoic acid	318 ± 2.7
2,4,6-trihydroxyacetophenone	317 ± 1.7

* From NIST electronic database (Bartmess, 1997), obtained from ion/molecule equilibrium measurements.

ganics, which generally have a PA above those of the matrices. Aromatic or oxygen-containing analytes may not have higher PAs than common matrices. Sensitivity for such analytes should then be improved by choosing a matrix with a lower PA.

For matrices with a low PA, and/or analytes with a high PA, the proton-transfer reaction will be quite exothermic. This excess energy will be deposited into the reaction partners as internal excitation, and can lead to increased analyte fragmentation (Tang et al., 1997; Gross et al., 1998; Jørgensen et al., 1998). Metastable fragmentation results of other authors can be understood in the same way, although different effective desorption temperatures may also be important (Karas et al., 1995). It has also been shown that a relatively low matrix PA led to increased multiply charged analyte, presumably by repeated protonation (Jørgensen et al., 1998).

Deprotonated matrix ions have gas-phase basicities (GBs) in the range from 344 kcal/mol for aromatic amines like 3-aminoquinoline to 316 kcal/mol for a phenolic ketone like 2,4,6 trihydroxyacetophenone (Table 5) (Breuker et al., 1998). It is interesting that the anion GB values follow the same general trend as the aqueous solution basicities; amines have larger values than ketones or acids. Use of a "basic" matrix may, thus, give the desired analyte anions, but, due to gas-phase rather than solution reactions:

$$(M - H)^- + A \rightarrow M + (A - H)^-$$

From the recently obtained GBs, it is clear that MALDI matrix anions are not generally capable of deprotonating many analyte classes, such as nitrogen-containing compounds, hydrocarbons, thiols, carbonyls, or alcohols (Harrison, 1992). It may, therefore, be the case that $(A\text{-}H)^-$ ions are often a result of dissociative electron capture reactions, as noted above for matrices.

3. Gas-Phase Cationization

Several studies of cationized molecules generated under MALDI conditions have shown that these ions, in many cases, result from ion–molecule reactions in the gas phase. This general idea has been around for a long time, and has, for example, been used to describe the pseudo-molecular ions formed by laser desorption mass spectrometry without matrix (van der Peyl et al., 1981; Cotter, 1987). Chemical ionization by metal cations is also widely researched in areas that are unrelated to MALDI (Eller & Schwarz, 1991). Often, such experiments have been carried out in ion traps that allow long reaction times. In MALDI, cations generally do not even need to be added to the sample: ubiquitous Na^+ and K^+ impurities are sufficient to give strong alkali cationized signals. To our knowledge, the formation of negative analyte adducts with small anions present in the plume has not been observed in MALDI.

Several recent studies have provided solid experimental data in support of gas-phase cationization processes in MALDI. Wang et al. (Wang et al., 1993) and Belov et al. (Belov et al., 1998) studied the formation of cationized peptides by additional laser irradiation of a neat NaI sample to generate free sodium ions in the source region of their instruments. These authors found a dramatic enhancement of the $(M+Na)^+$ peak of gramicidin S in the presence of the laser-generated sodium ions, compared to normal MALDI conditions. Using delayed ion extraction, Wang et al. (Wang et al., 1993) also found that the pseudo-molecular ion signals peaked at an optimum delay time of several 100 ns. These results were interpreted as evidence for gas-phase cationization reactions. Metal ion pick-up reactions are thought to be especially important in MALDI of synthetic polymers. Bowers and co-workers used ion chromatography to show that sodium ions can be very well "solvated" in the gas phase by polyethylene glycol oligomers (von Helden et al., 1995). Liao and Allison (Liao & Allison, 1995) also presented gas-phase capture of cations, in particular Na^+, as one possible mechanism among many others for pseudo-molecular ion formation in MALDI. They also caution that sample preparation has a strong influence on the presence or absence of cationized species in the mass spectra.

Addition of alkali matrix salts to MALDI samples has been found to be a way to cationize synthetic polymers (Dogruel et al., 1996). Inclusion of 10% of the sodium salt of DHB gave strong sodiated signals of poly(methyl methacrylate). Pure alkali salts of DHB used as matrix gave no analyte signal, despite a sufficiently strong UV absorption.

As with protons, affinities toward various cations can be determined using mass spectrometric methods. For sodium and potassium ions, some values are known from the work of Castleman (Guo et al., 1989) and Kebarle (Klassen et al., 1996). Cation affinites are generally in the range of about 25– 40 kcal/mol for small molecules, substantially smaller

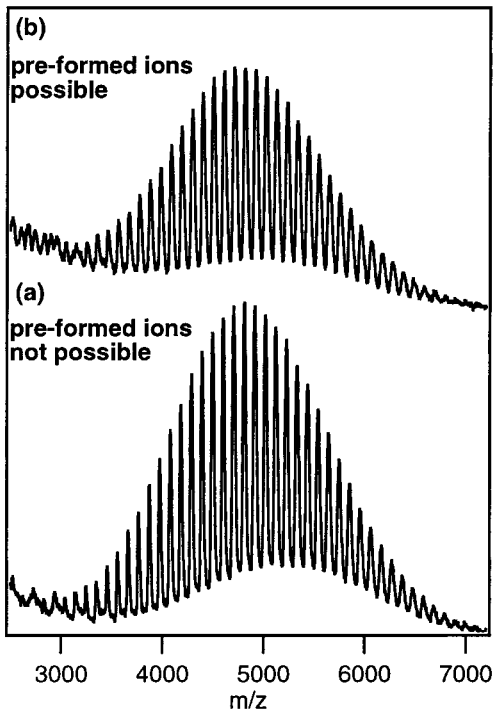

FIGURE 9. MALDI mass spectra of polystyrene 5000 with dithranol as a matrix and $Cu(TF)_2 \cdot H_2O$ as cationizing agent in molar ratio 1:114:2.9. In (a), dithranol and polystyrene 5000 were crystallized from THF, and $Cu(TFA)_2 \cdot H_2O$ dissolved in water was crystallized on top. Copper-polystyrene adducts cannot be pre-formed in solution. (b) Dithranol, polystyrene and $Cu(TFA)_2 \cdot H_2O$ cocrystallized from THF. Preformed copper-polystyrene adducts are possible. The laser power was the same for both spectra. (Copyright John Wiley & Sons, Ltd. Reproduced with permission from Lehmann et al., 1997.)

than the corresponding proton affinities. No clear correlation with proton affinities is found, except within limited sets of structurally similar compounds. Also, no information on cation affinities for species relevant to MALDI are available in the literature, with the exception of alkali ion affinities for glycine (ΔH_{298} = 37.5 kcal/mol for Na^+, 30.1 kcal/mol for K^+) and gly-gly (ΔH_{298} = 64.7 kcal/mol for Naq^+) reported by Kebarle (Klassen et al., 1996). All these values are much smaller than the corresponding proton affinites (see Table 4).

A particularly clear example where gas-phase cationization plays the dominant role is MALDI MS of polystyrene (PS). Like other apolar synthetic polymers, polystyrene is most easily detected if metal salts are added to the MALDI matrix. Polystyrene is readily cationized by copper or silver, forming singly charged ions in the spectrum (Llenes & O'Malley, 1992; Belu et al., 1996; Chowdhary et al., 1996; Deery et al., 1997; Mowat et al., 1997). Transition metals such as copper or silver are expected to bind to the phenylic π-system with electrons from the metal d-orbitals. Initially, it was unclear, however, whether such π-complexes are formed in the solid MALDI sample and desorbed, or whether they form exclusively in the gas phase. Furthermore, it was not known whether charge compensation for divalent transition metal cations occurred by deprotonation of polystyrene or by reduction of the metal ion. Experiments performed in our laboratory answered these questions (Lehmann et al., 1997). Layered sample preparations with two immiscible solvents were used that allowed separate depositions of the polystyrene/matrix mixture and of the cationization agent, a Cu(II) salt. Complex formation in the solid was, therefore, excluded. Nevertheless, strong signals of copper-cationized PS were observed, with intensities comparable to samples, where all sample compounds were crystallized together from the same solution (Fig. 9). This experiment suggested a gas-phase mechanism for the formation of the polystyrene pseudo-molecular ions.

Why is polystyrene cationized and not protonated? Assuming a proton affinity close to that of benzene (181 kcal/mol), protonation may indeed seem likely. We must, however, consider where the proton is coming from. A logical proton source would be the protonated matrix; for example, dithranol (PA = 209 kcal/mol), which is frequently used for MALDI of polystyrene. However, this process is endothermic: ΔH = PA (dithranol) − PA (benzene) = + 28 kcal/mol. On the other hand, cation affinities are much smaller. If, for example, a silver ion is transferred from silver-cationized matrix to polystyrene, the overall process may be close to thermoneutral. If silver attaches as a free ion in the gas phase, then an exothermic reaction is expected: the gas-phase binding energy of Ag^+ to benzene is 37 kcal/mol (Freiser, 1996). Other recent studies fully support the conclusion that gas-phase cationization is the dominant ionization pathway in MALDI of polystyrene (Hoberg et al., 1997; Burgers & Terlouv, 1998; Rashidezadeh & Guo, 1998). The question about the oxidation of the copper state was resolved by high-resolution mass spectrometry of some of the cationized oligomers (Zenobi, 1997). No deprotonation was observed, but cationization by Cu(I) was, even though Cu(II) was present in the sample. This clearly shows that the transition metal cation has undergone reduction, as discussed in Section III.B.5.

4. Electron Transfer

Electron transfer can become important for MALDI analysis of compounds with low ionization potentials (Juhasz & Costello, 1993; Lidgard & Duncan, 1995). Limbach and coworkers identified anthracene and terthiophene as electron transfer matrices for the analysis of ferrocene derivatives (McCarley et al., 1998). These authors propose resonant two-photon ionization of matrix, followed by electron transfer from analyte to the matrix radical cation. This process can happen only if the analyte has a lower ionization potential than the matrix (IP of anthracene = 7.44 eV, IP of ferrocene = 6.71 eV (Lias et al., 1998)):

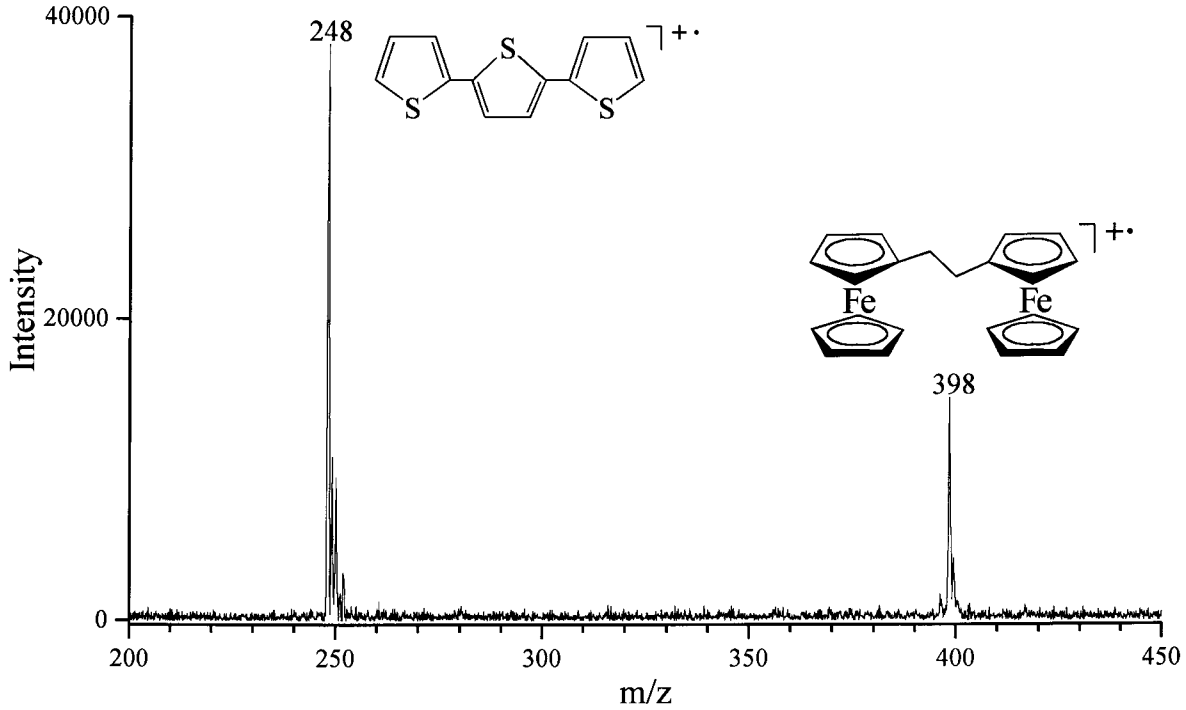

FIGURE 10. MALDI analysis of 1,2-diferrocenylethane, using a 1000-fold excess of terthiophene as an electron transfer matrix (Reprinted with permission from McCarley et al., 1998. Copyright 1998 American Chemical Society.)

$$M^{+\bullet} + A \rightarrow M + A^{+\bullet} \quad IP(M) > IP(A).$$

Control experiments excluded the direct photoionization of analyte, as well as a mechanism where the matrix served only to assist in the desorption of the analyte. The highest mass compound analyzed in this way was a dendrimer containing a ferrocene core, with a molecular weight of over 5000 Da. Figure 10 shows an example, the analysis of octa (ferrocenyl dimethyl silane) using anthracene as a matrix.

In this case, electron transfer was intentionally enhanced, but such reactions are not otherwise commonly observed. The reason for this finding is that typical UV MALDI matrices have low IPs, as discussed in Section III.A.2. Of the amino acids whose IPs are known, only that of tryptophan lies below that of DHB (Lias et al., 1998); thus, the corresponding electron transfer reactions are thermodynamically unfavorable. This is consistent with the fact that peptides are commonly observed in MALDI as protonated adducts rather than radical cations.

Electron-transfer reactions can also be a mechanism by which ions are neutralized in the plume or even in the flight tube. As has been shown for MALDI-generated protonated proteins, collisions with inert gases at the keV energies (lab frame) used in TOF-MS can result in substantial charge exchange and signal loss (Giannakopulos et al., 1996):

$$MH^+ + R \rightarrow M + H + R^+$$

where R is the collision partner. In addition to inert gases, water or air could be expected to be equally effective in this reaction, as was shown for NO. This process is an additional reason to operate TOF mass spectrometers at low pressures.

5. *Charge Compensation*

For analytes up to a few 1000 Da, multiply charged ions are not common in MALDI. Ions of rather surprising composition are observed with a net charge of only one. These ions are typically adducts, often of divalent metal ions. For example, ions of the nominal composition $(DHB_nCa_{n-1})^+$ have been observed for n up to 6 (Dubois et al., 1996). High-resolution mass spectrometry showed that, to achieve the net charge of one, two protons were lost for every Ca^{2+} ion incorporated. A similar observation has been made by Wong and Chan (Wong & Chan, 1997), who found that cationization of polar polymers with di- and trivalent metal ions always resulted in singly charged pseudo-molecular ions in the mass spectrum. Charge compensation was via deprotonation or complexation with deprotonated matrix. At about 0.3-nm distance, two like charges have a Coulomb energy equivalent to a typical CH or OH bond energy. Therefore, the protons could, in principle, be ejected into the gas phase. However, the reaction is likely to occur earlier during desorption as the ions become desolvated. The effect is neither limited to matrix complexes, nor to positive ions.

TABLE 6. Mechanistic Summary: Primary and secondary ionization mechanisms discussed in the text, and their activities in different forms of MALDI.

	UV MALDI			IR MALDI	2-Phase MALDI
	P+	NP+	P−	P/NP	+/−
Primary					
MPI	●	●	●		
Pooling	●●	●●	●●	??	
ESPT	?		??		
Disproportionation	??		??		??
Performed	●●	●	●	●●	●●
Thermal				?	●●
Spallation				??	
Secondary					
H^+ Transfer	●●		●●	●●	●●
e^- Capture & H^+ Transfer			●●		
Cationization	●●	●●		●●	●●
e^- Transfer	●	●	??		
Ejection	●		●		

UV = ultraviolet excitation, IR = infrared excitation. Polarity of observed ions is indicated by + or −. P = polar analytes, NP = non-polar analytes. ●● = probably highly active, or active in many cases; ● = probably active, or active in some cases; ? = possibly sometimes active; ?? = possibly active, but not well-studied. No entry indicates probable lack of activity. MPI = multiphoton ionization, ESPT = excited-state proton transfer. Due to relative lack of experimental data, the UV NP− and IR− categories are not included, although the conclusions for IR+ may carry over to IR− with little change.

For example, a peptide anion of composition $(A+2Na+K-4H)^-$ has been observed by Fitzgerald, et al. (Fitzgerald et al., 1993). It seems very likely that these ions are the result of multiple collisions in the plume. Attachment of each additional metal ion is followed by loss of protons, and the process repeats.

In other cases, the divalent metal ions are apparently simply reduced. An example is cationization of styrene pentamers by Cu^{2+} salts, where only singly charged adducts were observed (Lehmann et al., 1997; Zenobi, 1997). High-resolution mass spectrometry showed that the net charge of one was not achieved by proton loss. The source of electrons may have been photoionized matrix. Under continuous extraction conditions, electrons are available for only a short time; thus, this alone seems unlikely to account for the complete absence of divalent complexes. Because divalent metal ions in the gas phase have high electron affinities (Cu^{2+} = 20.292 eV), (Lide, 1992), electron transfer from matrix or analyte in a collision becomes energetically favorable as the ions become desolvated during desorption. A second electron will not be transferred, because the first metal IPs are too low (Cu^+ = 7.726 eV).

IV. SUMMARY AND OUTLOOK

We have shown that one should not be tempted to describe the MALDI process in an oversimplified manner. Nevertheless, enough data have accumulated recently to significantly constrain the mechanistic possibilities. Based on these data, some typical MALDI experiments such as gas-phase protonation, gas-phase deprotonation, or gas-phase cationization can now be more accurately described. In other cases, however, many different proposed mechanisms are possible. Opportunities, therefore, remain for further study. For example, little is presently known about disproportionation and spallation as mechanisms for primary ion formation.

Table 6 presents an overview of the contribution of the primary and secondary ionization mechanisms to the formation of matrix and analyte ions by MALDI. Table 7 summarizes our conclusions differently, by listing the important ionic products for different analyte classes originating from the different ionization pathways.

What are the possibilities for better control of MALDI experiments? As a result of better knowledge about the ion formation process, a number of practically applicable strategies can be presented.

A. Control of Fragmentation

The energy liberated by gas-phase proton transfer reactions can greatly influence fragmentation. For oligonucleotides, Zhu et al. (Zhu et al., 1995) have proposed that the loss of protonated base, followed by backbone fragmentation and disproportionation, ultimately leads to anionic fragments. Consequently, the difference in proton affinity between analyte and matrix should determine the energy available. For

TABLE 7. Ions from selected classes of analytes, formed by primary and secondary MALDI ionization processes.

	Desorption of pre-formed ions	Gas-phase proton transfer	Gas-phase cationization, anion addition	Electron transfer	Charge ejection
Peptides, proteins	tagged: A^+	**$(A + H)^+$** $(A - H)^-$	$(A + C)^+$		$(A + C(II) - H)^+$
Metalloproteins	**$(A + C)^+$**	$(A + H)^+$ $(A - H)^-$	**$(A + C)^+$**		$(A + C(II) - H)^+$
Ionophores, Metal complex ligands	**$(A + C)^+$**	$(A + H)^+$ $(A - H)^-$	**$(A + C)^+$**		$(A + C(II) - H)^+$
Oligonucleotides		$(A + H)^+$ **$(A - H)^-$**	$(A + Na/K)^+$		
Oligosaccharides		$(A - H)^-$	**$(A + C)^+$** $(A + Na/K)^+$		$(A + C - nH)^-$
Polar Polymers		$(A + H)^+$ $(A - H)^-$	**$(A + Na)^+$** **$(A + K)^+$** $(A + C)^+$		$(A + C(II) - H)^+$
Apolar Polymers			**$(A + C)^+$** $(A + Ag)^+$		$(A + C(II) - H)^+$
Fullerenes, Fullerene Derivatives		$(A + H)^+$ $(A - H)^-$	$(A + C)^+$	$A^{+\bullet}$ **$A^{+\bullet}$**	
Low-IP compounds (e.g. Ferrocenes, metallocycles)				**$A^{+\bullet}$** $A^{-\bullet}$	
Highly acidic analytes (e.g. sulfonated dyes)	$(A - H)^-$	$(A - H)^-$	$(A + X)^-$		

Products from dominant processes are in boldface. A = analyte, C = metal cation (sometimes specified as Na, K, Ag . . .), X = counter anion.

reducing fragmentation of oligodeoxynucleotides, matrices with relatively high proton affinities should, therefore, be chosen.

Excess energy released by proton transfer is, however, not the only factor in fragmentation control. As noted in Section II.C, the sublimation temperature of matrices influences the internal energies of analytes (Mowry & Johnston, 1994; Karas et al., 1996). This can lead to fragmentation trends that are inversely correlated with proton affinities. For example, Karas et al. (Karas et al., 1995) have found that, for protonated glycoproteins, post-source decay follows the order SA < DHB < 3HPA, in agreement with Spengler et al. (Spengler et al., 1992), who also described SA as a "hotter" matrix than DHB. However, the order of the proton affinities is just the opposite: DHB (204 kcal/mol) < SA (210 kcal/mol) < HPA (214 kcal/mol). Plume processes are also known to contribute to fragmentation. As discussed in Section II.C, high extraction fields or regions of relatively high gas pressure can be chosen to increase fragmentation; both increase PSD through collisional effects.

B. Derivatization Strategies for Enhancement of Ion Yields

Difficult analytes will always exist. From the range of mechanistic possibilities presented here, it is clear that MALDI cannot be a universal method. Problem analytes, can, however, be made more amenable to MALDI analysis. Development of derivatization methods for classes of analytes could open new horizons for MALDI. Any of the mechanisms described can be used as a design goal. A potential extra benefit of good derivatization strategies is that they could reduce discrimination effects in multicomponent analysis. If, for example, all analytes have the same attached group of high proton or cation affinity, then there is less reason for competition problems to appear. Derivatization could simultaneously be used to enhance incorporation into the matrix.

Synthetic attachment of a "charge tag" is an example of successful use of this strategy. Claereboudt et al. (Claereboudt et al., 1993) as well as Allison and coworkers (Liao &

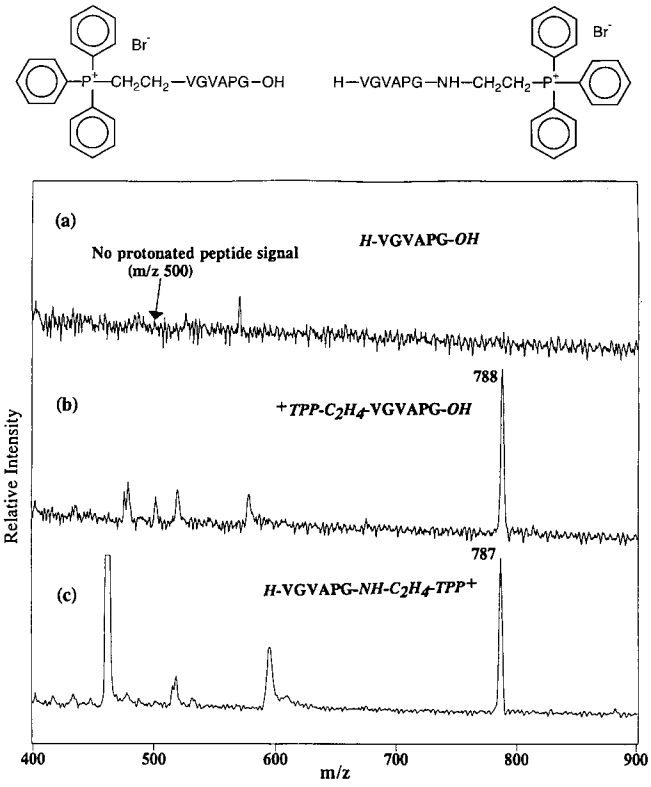

FIGURE 11. Portions of the MALDI mass spectra for the peptide H-VGVAPG-OH (molecular weight 498.6). Top panel: chemical structures — phosphonium ion derivatives of the peptide H-VGVAPG-OH. Bottom panel: MALDI mass spectra of (a) underivatized peptide; (b) N-terminal ethyltriphenylphosphonium derivative; (c) C-terminal aminoethyl triphenylphosphonium derivative. The same matrix, 4HCCA, and the same laser power were used to obtain each spectrum. (Copyright John Wiley & Sons, Ltd. Reproduced with permission from Liao & Allison, 1995.)

Allison, 1995) (Fig. 11) have found an increased signal of phosphonium derivativized compounds. A significant secondary benefit of this strategy is that it allows for direct MALDI analysis of derivatized peptides in polyacrylamide gels (Strahler et al., 1997).

Gut et al. (Gut et al., 1997) used a charge-tagging approach by derivatizing DNA with a quarternary ammonium functionality. They reported a 100-fold improvement in detectability. Naven and Harvey (Naven & Harvey, 1996) used Girard's T reagent to derivatize oligosaccharides in a similar manner. Spengler and coworkers (Spengler et al., 1997) have used related chemistry for localizing the charge after PSD of peptides in MALDI experiments, facilitating primary structure elucidation.

C. Control of Charge State

As shown by Jørgensen et al. (Jørgensen et al., 1998), a correlation exists between the proton affinity of the matrix and the abundance of multiply charged analyte ions, such as insulin and myoglobin. This correlation also implies that these protein ions are largely formed by reactions with protonated matrix. Owing to electrostatic repulsion, the analyte proton affinity decreases as the number of charges increases; however, for large proteins, the proton affinity of the protonated molecule can still be quite high. In the experiment described by Jørgensen, the intensity of the doubly charged insulin ion was larger if 4HCCA (PA = 202 kcal/mol) rather than sinapic acid (PA = 210 kcal/mol) was used. The proton transfer from $(\text{matrix}+\text{H})^+$ to analyte is ≈ 8 kcal/mol more exothermic for the 4HCCA matrix; that difference explains why this matrix is better able to further protonate the $(\text{insulin}+\text{H})^+$ ion. In general, the lower the proton affinity of the matrix molecule, the greater the chance for observing doubly or multiply protonated analyte.

For cases where analyte ions are not formed by gas-phase protonation, such a straightforward dependence on proton affinity cannot be expected. Also, other experimental conditions, notably the sample preparation, can influence the relative intensity of multiply charged ions.

D. Guidelines for Matrix Selection

Difficulties with MALDI analyses can stem from many sources, not only ionization problems. Incorporation of analyte into a solid matrix and formation of suitable matrix crystallites are among the most frequent. However, knowledge about ion formation pathways can now contribute to rational matrix selection. The fundamental consideration is the type of analyte ion expected or desired.

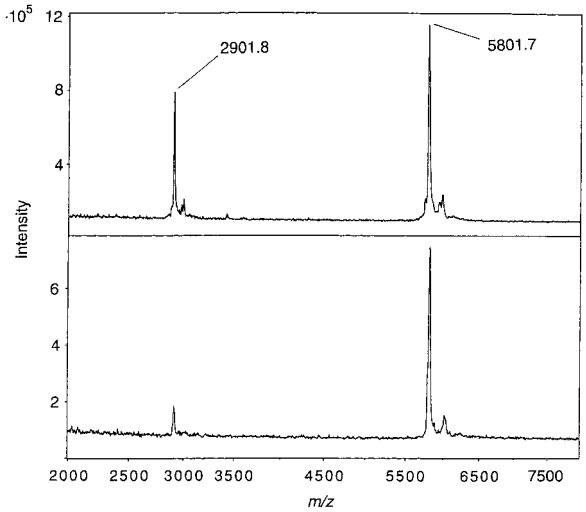

FIGURE 12. MALDI spectra of insulin with two different MALDI matrices. Upper spectrum, 4HCCA; lower spectrum, sinapic acid. The peaks at *m/z* 5801.7 and *m/z* 2901.8 can be assigned to the MH^+ and MH^{2+} ions. Small peaks from adducts of insulin and the matrix are also observed. (Reprinted by permission of I.M. Publications from Jørgensen et al., 1998. Copyright I.M. Publications 1998.)

Given some chemical intuition or prior knowledge of the acidity or basicity of the proposed analyte, secondary protonation or deprotonation reactions can be enhanced by selecting a matrix with the appropriate PA or GB, using the tables presented here. This may be the most important and yet easiest type of optimization that can be carried out for UV MALDI. This parameter also is relevant for controlling the degree of analyte fragmentation, as noted above.

If cationized analytes are desired or expected, then the matrix should be chosen so as not to compete with analyte for the selected cations in the condensed or in the gas phase. Matrices that are good complexing agents, such as those with ortho-hydroxy carbonyl units, should probably be avoided or derivatized. Classes of metal ions can be selected for their likely binding strength to the analytes, although an exact correlation with solution-phase association constants is not expected in MALDI. Bulky counter-ions should reduce Coulomb forces and increase net ion yields. Divalent cations are probably preferable in general, due to higher electrostatic binding energies.

If the analyte can be expected to have a low IP (metallocenes, fullerenes, extended conjugated systems, etc.), the formation of analyte radical cations can be enhanced by selection of a matrix with a higher IP. In this case, using a laser with high photon energy to perform direct MPI of the matrix will also be helpful.

E. Guidelines for Matrix Design

Each of the primary ionization mechanisms discussed can be used as a design criterion for new matrices. Lower matrix IPs might provide greater initial ion density by two-photon ionization. Known trends in gas-phase ion properties can be used to design matrices with very high proton affinities or basicities. Selection of matrices that have large exciton interactions or exciton mobilities in the solid should enhance pooling or disproportionation ionization. A search could be made for ESPT molecules that retain activity under conditions expected in MALDI matrix solids, or a mixed matrix could be developed to provide a suitable ESPT environment. Conversely, matrices could be found with enhanced excited-state basicity. In two-phase MALDI, even finer particulates should be developed, and attention given to increasing the work function of the surface, or decreasing the IP of the liquid.

A main goal of matrix design must be to improve the number of primary ions that are created per input photon. As we have seen, however, desorption very likely contributes in an important way to the final separation of the initial ions so that they can be detected. Extra consideration could be given to improving this part of the combined process, possibly by the choice of co-matrices that yield good plume characteristics and a low fraction of large clusters and chunks.

ACKNOWLEDGMENTS

We thank Kathrin Breuker, Klaus Dreisewerd, and Martin Schär for many helpful comments, and the following people for providing figures for this review: J. Allison, B. Chait, G. Bojesen, F. Hillenkamp, G. Kinsel, P. Limbach, and B. Spengler.

REFERENCES

1. Aksouh, F. et al. Influence of the laser-beam direction on the molecular ion ejection angle in matrix-assisted laser desorption/ionization. Rapid Commun Mass Spectrom 1995, 9, 515.
2. Allwood, D. A.; Dyer, P. E.; Dreyfus, R. W. Ionization modeling of matrix molecules in ultraviolet matrix-assisted laser desorption/ionization. Rapid Commun Mass Spectrom 1997, 11, 499.
3. Allwood, D. A.; Dyer, P. E.; Dreyfus, R. W.; Perera, I. K. Plasma modeling of matrix-assisted UV laser-desorption/ionization (MALDI). Appl Surf Sci 1997, 110, 616.
4. Bartmess, J. E. Negative Ion Energetics Data, NIST Standard Reference Database No. 69, Vol. August; National Institute of Standards and Technology: Gaithersburg, MD 20899 (http://webbok.nist.gov), 1997.
5. Beavis, R. C. Phenomenological models for matrix-assisted laser desorption ion yields near the threshold fluence. Org Mass Spectrom 1992, 27, 864.
6. Beavis, R. C.; Chait, B. T. Factors affecting the ultraviolet laser desorption of proteins. Rapid Commun Mass Spectrom 1989, 3, 233.
7. Beavis, R. C.; Chait, B. T. Velocity distributions of intact high mass polypeptide molecule ions produced by matrix-assisted laser desorption. Chem Phys Lett 1991, 181, 479.
8. Becker, C. H.; Jusinski, L. E.; Moro, L. Infrared laser-induced desorption of neutral organic compounds from frozen aqueous solution followed by single-photon ionization. Int J Mass Spectrom Ion Proc 1990, 95, R1.
9. Belov, M. E.; Myatt, C. P.; Derrick, P. J. Chemical ionization of neutral peptides produced by matrix-assisted laser desorption. Chem Phys Lett 1998, 284, 412.
10. Belu, A. M.; De Simone, J. M.; Linton, R. W.; Lange, G. W.; Friedman, R. M. Evaluation of matrix-assisted laser desorption/ionization mass spectrometry for polymer characterization. J Am Soc Mass Spectrom 1996, 7, 11.
11. Berkenkamp, S.; Karas, M.; Hillenkamp, F. Ice as a matrix for IR-matrix-assisted laser desorption/ionization—Mass-spectra from a protein single-crystal. Proc Nat Acad Sci USA.1996, 93, 7003.
12. Berkenkamp, S.; Kirpekar, F.; Hillenkamp, F. Infrared MALDI mass spectrometry of large nucleic acids. Science 1998, 281, 260.
13. Berkenkamp, S.; Menzel, C.; Karas, M.; Hillenkamp, F. Performance of infrared matrix-assisted laser desorption/ioniza-

tion mass spectrometry with lasers emitting in the 3 μm wavelength range. Rapid Commun Mass Spectrom 1997, 11, 1399.

14. Bökelmann, V.; Spengler, B.; Kaufmann, R. Dynamical parameters of ion ejection and ion formation in matrix-assisted laser desorption/ionization. Eur Mass Spectrom 1995, 1, 81.
15. Breuker, K.; Knochenmuss, R.; Zenobi, R. The gas-phase basicities of deprotonated MALDI matrix molecules. Int J Mass Spectrom Ion Proc, to appear.
16. Burgers, P. C.; Terlouv, J. K. Monoisotopic $^{65}Cu^{+}$ attachment to polystyrene. Rapid Commun Mass Spectrom 1998, 12, 801.
17. Burton, R. D.; Watson, C. H.; Eyler, J. R.; Lang, G. L.; Powell, D. H.; Avery, M. Y. Proton affinities of 8 matrices used for matrix-assisted laser desorption/ionization. Rapid Commun Mass Spectrom 1997, 11, 443.
18. Calba, P. J.; Muller, J. F.; Hachimi, A. P. L.; Guglielmetti, R. Spirooxazines as a molecular probe for the study of matrix-assisted laser desorption/ionization processes. Part I: Study of the interaction effect between the molecular probe and the matrix. Rapid Commun Mass Spectrom 1997, 11, 1602.
19. Caldwell, K. L.; Murray, K. K. Mid-infrared matrix-assisted laser desorption/ionization with a water/glycerol matrix. Appl Surf Sci 1998, 127–129, 242.
20. Caprioli, R. M.; Malorni, A.; Sidona, G. Mass Spectrometry in Biomolecular Sciences, NATO ASI Ser. C, Vol. 475; Kluwer: Dordrecht, The Netherlands, 1996.
21. Carr, S. R.; Cassidy, C. J. J Gas-phase basicities of histidine and lysine and their selected di- and tripeptides. Am Soc Mass Spectrom 1996, 7, 1203.
22. Chan, T.–W. D.; Colburn, A. W.; P.J., D. Matrix-assisted laser desorption/ionization using a liquid matrix: Formation of high-mass cluster ions from proteins. Org Mass Spectrom 1992, 27, 53.
23. Chan, T. W. D.; Thomas, I.; Colburn, A. W.; Derrick, P. J. Initial velocities of positive and negative protein molecule-ions produced in matrix-assisted ultraviolet-laser desorption using a liquid matrix. Chem Phys Lett 1994, 222, 579.
24. Chapman, J. R. Protein and Peptide Analysis by Mass Spectrometry. Methods Mol. Biol., Vol. 61; Humana Press: Totowa, NJ, 1996.
25. Chen, X.; Carroll, J. A.; Beavis, R. C. Near-ultraviolet-induced matrix-assisted laser desorption/ionization as a function of wavelength. J Am Soc Mass Spectrom 1998, 9, 885.
26. Chevrier, M. R.; Cotter, R. J. A Matrix-assisted laser desorption time-of-flight mass spectrometer based on a 600 ps, 1.2 mL nitrogen laser. Rapid Commun Mass Spectrom 1991, 5, 611.
27. Chiarelli, M. P.; Sharkey, A. G.; Hercules, D. M. Excited-state proton transfer in laser mass spectrometry. Anal Chem 1993, 65, 307.
28. Chowdhary, A. K.; Critchley, G.; Diaf, A.; Beckmann, E. J.; Russell, A. J. Characterization of synthetic polymers using matrix-assisted laser desorption/ionization time of flight mass spectrometry. Macromol 1996, 29, 2213.
29. Claereboudt, J.; Claeys, M.; Geise, H.; Gijbels, R.; Vertes, A. Laser microprobe mass spectrometry of quarternary phosphonium salts: Direct versus matrix-assisted laser desorption. J Am Soc Mass Spectrom 1993, 4, 798.
30. Cornett, D. S.; Duncan, M. A.; Amster, I. J. Matrix-assisted laser desorption at visible wavelengths using a 2-component matrix. Org Mass Spectrom 1992, 27, 831.
31. Cornett, D. S.; Duncan, M. A.; Amster, I. J. Liquid-mixtures for matrix-assisted laser-desorption. Anal Chem 1993, 65, 2608.
32. Cotter, R. J. Laser mass spectrometry: An overview of techniques, instruments and applications. Anal Chim Acta 1987, 195, 45.
33. Cramer, R.; Haglund Jr., R. F.; Hillenkamp, F. Matrix-assisted laser desorption and ionization in the O—H and C═O absorption bands of aliphatic and aromatic matrices: Dependence on laser wavelength and temporal beam profile. Int J Mass Spectrom Ion Proc 1997, 169/170, 51.
34. Dai, Y.; Whittal, R. M.; Bridges, C. A.; Isogai, Y.; Hindsgaul, O.; Li, L. Matrix-assisted laser desorption/ionization mass spectrometry for the analysis of monosulfated oligosaccharides. Carbohydr Res 1997, 304, 1.
35. Dale, M. J.; Knochenmuss, R.; Zenobi, R. Graphite/liquid mixed matrices for laser desorption/ionization mass spectrometry. Anal Chem 1996, 68, 3321.
36. Dale, M. J.; Knochenmuss, R.; Zenobi, R. Two-phase MALDI-matrix selection and sample pretreatment for complex anionic analytes. Rapid Commun Mass Spectrom 1997, 11, 136.
37. Deery, M. J. et al. A study of cation attachment to polystyrene by means of matrix-assisted laser desorption/ionization and electrospray ionization mass spectrometry. Rapid Commun Mass Spectrom 1997, 11, 57.
38. Demirev, P. et al. Matrix-assisted laser desorption with ultrashort laser pulses. Rapid Commun Mass Spectrom 1992, 6, 187.
39. Dlott, D. D.; Hambir, S.; Franken, J. The new wave in shock waves. J Phys Chem B 1998, 102, 2121.
40. Dogruel, D.; Nelson, R. W.; Williams, P. The effects of matrix pH and cation availability on the matrix-assisted laser desorption/ionization mass spectrometry of poly(methyl metacrylate). Rapid Commun Mass Spectrom 1996, 10, 801.
41. Dougherty, D.; Younathan, E. S.; Voll, R.; Abdulnur, S.; McGlynn, S. P. Photoelectron spectroscopy of some biological molecules. J Electron Spectrosc Relat Phenom 1978, 13, 379.
42. Dreisewerd, K.; Schürenberg, M.; Karas, M.; Hillenkamp, F. Influence of the laser intensity and spot size on the desorption of molecules and ions in matrix-assisted laser-desorption/ionization with a uniform beam profile. Int J Mass Spectrom Ion Proc 1995, 141, 127.
43. Dreisewerd, K.; Schurenberg, M.; Karas, M.; Hillenkamp, F. Matrix-assisted laser desorption/ionization with nitrogen lasers of different pulse widths. Int J Mass Spectrom Ion Proc 1996, 154, 171.
44. Dubois, F.; Knochenmuss, R.; Steenvoorden, R. J. J. M.; Breuker, K.; Zenobi, R. On the mechanism and control of

salt-induced resolution loss in matrix-assisted laser desorption/ionization. Eur Mass Spectrom 1996, 2/3, 167.

45. Ehring, H.; Costa, C.; Demirev, P. A.; Sundqvist, B. U. R. Photochemical versus thermal mechanisms in matrix-assisted laser desorption/ionization probed by back side desorption. Rapid Commun Mass Spectrom 1996, 10, 821.
46. Ehring, H.; Karas, M.; Hillenkamp, F. Role of photoionization and photochemistry in ionization processes of organic molecules and relevance for matrix-assisted laser desorption/ionization mass spectrometry. Org Mass Spectrom 1992, 27, 427.
47. Ehring, H.; Sundqvist, B. U. R. Studies of the MALDI process by luminescence spectroscopy. J Mass Spectrom 1995, 30, 1303.
48. Ehring, H.; Sundqvist, B. U. R. Excited-state relaxation processes of MALDI-matrices studied by luminescence spectroscopy. Appl Surf Sci 1996, 96–98, 577.
49. Eller, K.; Schwarz, H. Organometallic chemistry in the gas phase. Chem Rev 1991, 91, 1121.
50. Ens, W.; Mao, Y.; Mayer, F.; Standing, K. G. Properties of matrix-assisted laser desorption. Measurements with a time-to-digital converter. Rapid Commun Mass Spectrom 1991, 5, 117.
51. Fitzgerald, M. C.; Parr, G. R.; Smith, L. M. Basic matrices for the matrix-assisted laser-desorption/ionization mass-spectrometry of proteins and oligonucleotides. Anal Chem 1993, 65, 3204.
52. Freiser, B. S. Organometallic Ion Chemistry; Kluwer: Dordrecht, 1996.
53. Fujii, T. Surface ionization organic mass spectrometry: Mechanism. Eur Mass Spectrom 1996, 2, 91.
54. Gallagher, J. W.; Brion, C. E.; Samson, J. A. R.; Langhoff, P. W. Absolute cross sections for molecular photoabsorption, partial photoionization, and ionic photofragmentation processes. J Phys Chem Ref Data 1988, 17, 9.
55. Giannakopulos, A. E.; Andersen, U. N.; Christie, J. R.; Reynolds, D. J.; Derrick, P. J. Charge transfer in collisions between gaseous protein ions and inert gases. Eur Mass Spectrom 1996, 2, 15.
56. Gimon, M. E.; Preston, L. M.; Solouki, T.; White, M. A.; Russell, D. H. Are proton transfer reactions of excited states involved in UV laser desorption/ionization? Org Mass Spectrom 1992, 27, 827.
57. Gimon–Kinsel, M.; Preston–Schaffter, L. M.; Kinsel, G. R.; Russell, D. H. Effects of matrix structure/acidity in ion formation in matrix-assisted laser desorption/ionization mass spectrometry. J Am Chem Soc 1997, 119, 2534.
58. Grigorean, G.; Carey, R. I.; Amster, I. J. Studies of exchangeable protons in the matrix-assisted laser desorption/ionization process. Eur Mass Spectrom 1996, 2, 139.
59. Gross, J. et al. Investigations of the metastable decay of DNA under ultraviolet matrix-assisted laser desorption/ionization conditions with post-source-decay analysis and hydrogen/deuterium exchange. J Am Soc Mass Spectrom 1998, 9, 866.
60. Guo, B. C.; Conklin, B. J.; Castleman, A. W. Thermochemical properties of ion complexes $Na^+(M)_n$ in the gas phase. J Am Chem Soc 1989, 111, 6506.
61. Gut, I. G.; Jeffery, W. A.; Pappin, D. J. C.; Beck, S. Analysis of DNA by "charge tagging" and matrix-assisted laser desorption/ionization mass spectrometry. Rapid Commun Mass Spectrom 1997, 11, 43.
62. Hahndschuh, M.; Nettesheim, S.; Zenobi, R. Laser-induced molecular desorption and particle ejection from organic films. Appl Surf Sci, to appear.
63. Harrison, A. G. Chemical Ionization Mass Spectrometry; CRC Press: Boca Raton, 1992.
64. Harrison, A. G. The gas-phase basicities and proton affinities of amino acids and peptides. Mass Spectrom Rev 1997, 16, 201.
65. Heise, T. W.; Yeung, E. S. Dynamics of matrix-assisted laser desorption as revealed by the associated acoustic signal. Anal Chim Acta 1995, 199, 377.
66. Hellwege, K–H. Einführung in die Festkörperphysik; Springer–Verlag: Berlin, 1988.
67. Hillenkamp, F.; Karas, M.; Beavis, R. C.; Chait, B. T. Matrix-assisted laser desorption/ionization mass spectrometry of biopolymers. Anal Chem 1991, 63, 1193A.
68. Hoberg, A.–M.; Haddleton, D. M.; Derrick, P. M. Evidence for cationization of polymers in the gas phase during matrix-assisted laser desorption/ionization. Eur Mass Spectrom 1997, 3, 471.
69. Hunter, J. M.; Lin, H. A.; Becker, C. H. Cryogenic frozen solution matrices for analysis of DNA by time-of-flight mass-spectrometry. Anal Chem 1997, 69, 3608.
70. Huth–Fehre, T.; Becker, C. H. Energetics of gramicidin S after UV laser desorption from a ferrulic acid matrix. Rapid Commun Mass Spectrom 1991, 5, 378.
71. Ireland, J. F.; Wyatt, P. A. H. Acid-base properties of electronically excited states of organic molecules. Adv Phys Org Chem 1976, 12, 131.
72. Israelachvili, J. Intermolecular and Surface Forces; Academic: London, 1991.
73. Johnson, R. E. Models for matrix-assisted desorption by a laser-pulse. Int J Mass Spectrom Ion Proc 1994, 139, 25.
74. Johnson, R. E. Models for matrix-assisted laser desorption and ionization: MALDI. In: Large ions: Their vaporization, detection and structural analysis; T. Baer; C. Y. Ng;I. Powis (Eds.); Wiley: New York, 1996, 49.
75. Johnson, R. E.; Sunqvist, B. U. R Laser pulse ejection of organic molecules from a matrix: Lessons from fast-ion-induced ejection. Rapid Commun Mass Spectrom 1991, 5, 574.
76. Jørgensen, T. J. D.; Bojesen, G.; Rahbek–Nielsen, H. The proton affinities of seven matrix-assisted laser desorption/ionization matrices correlated with the formation of multiply charged ions. Eur Mass Spectrom 1998, 4, 39.
77. Jouvet, C.; Lardeux–Dedonder, C.; Richard–Viard, M.; Solgadi, D.; Tramer, A. Reactivity of molecular clusters in the gas phase. Proton-transfer reactions in neutral phenol-$(NH_3)_n$ and phenol-$(C_2H_5NH_2)_n$. J Phys Chem 1990, 94, 5041.
78. Juhasz, P.; Biemann, K. Mass spectrometric molecular-weight

determination of highly acidic compounds of biological significance via their complexes with basic polypeptides. Proc Natl Acad Sci USA 1994, 91, 4333.

79. Juhasz, P.; Costello, C. E. Generation of large radical ions from oligometallocenes by matrix-assisted laser desorption/ionization. Rapid Commun Mass Spectrom 1993, 7, 343.
80. Juhasz, P.; Costello, C. E.; Biemann, K. Matrix-assisted laser desorption/ionization mass-spectrometry with 2-(4-hydroxyphenylazo)benzoic acid matrix. J Am Soc Mass Spectrom 1993, 4, 399.
81. Juhasz, P.; Vestal, M. L.; Martin, S. A. On the initial velocity of ions generated by matrix-assisted laser-desorption/ionization and its effect on the calibration of delayed extraction time-of-flight mass-spectra. J Am Soc Mass Spectrom 1997, 8, 209.
82. Karas, M.; Bachmann, D.; Bahr, U.; Hillenkamp, F. Matrix-assisted ultraviolet laser desorption of non-volatile compounds. Int J Mass Spectrom Ion Proc 1987, 78, 53.
83. Karas, M.; Bachmann, D.; Hillenkamp, F. Influence of the wavelength in high-irradiance ultraviolet laser desorption mass spectrometry of organic molecules. Anal Chem 1985, 57, 2935.
84. Karas, M.; Bahr, U.; Stah–Zeng, J. R. Steps toward a more refined picture of the matrix function in UV MALDI. In: Large Ions: Their Vaporization, Detection and Structural Analysis; T. Baer; C. Y. Ng; I. Powis (Eds.); Wiley: London, 1996, 27.
85. Karas, M.; Bahr, U.; Strupat, K.; Hillenkamp, F.; Tsarbopoulos, A.; Pramanik, B. N. Matrix dependence of metastable fragmentation of glycoproteins in MALDI TOF mass-spectrometry. Anal Chem 1995, 67, 675.
86. Karas, M. et al. Matrix-assisted laser-desorption/ionization mass-spectrometry with additives to 2,5-dihydroxybenzoic acid. Org Mass Spectrom 1993, 28, 1476.
87. Karas, M.; Hillenkamp, F. Laser desorption ionization of proteins with molecular masses exceeding 10,000 daltons. Anal Chem 1988, 60, 2299.
88. Karbach, V.; Knochenmuss, R. Do single matrix molecules generate primary ions in ultraviolet matrix-assisted laser desorption/ionization? Rapid Commun Mass Spectrom 1998, 12, 968.
89. Kinsel, G. R.; Edmondson, R. D.; Russell, D. H. Profile and flight time analysis of bovine insulin clusters as a probe of matrix-assisted laser desorption/ionization ion formation dynamics. J Mass Spectrom 1997, 32, 714.
90. Klassen, J. S.; Anderson, S. G.; Blades, A. T.; Kebarle, P. Reaction enthalpies for $M + L = M^+ + L$, where $M^+ = Na^+$ and K^+ and L = acetamide, N-methylacetamide, N,N-dimethylacetamide, glycine, and glycylglycine, from determinations of the collision-induced dissociation thresholds. Phys Chem 1996, 100, 14218.
91. Knochenmuss, R.; Dubois, F.; Dale, M. J.; Zenobi, R. The matrix suppression effect and ionization mechanisms in matrix-assisted laser desorption/ionization. Rapid Commun Mass Spectrom 1996, 10, 871.
92. Knochenmuss, R.; Karbach, V.; Wiesli, U.; Breuker, K.; Zenobi, R. The matrix suppression effect in matrix-assisted laser desorption/ionization: Application to negative ions and further characteristics. Rapid Commun Mass Spectrom 1998, 12, 529.
93. Knochenmuss, R.; Leutwyler, S. Proton transfer reactions in neutral gas-phase clusters: 1-naphthol with H_2O, D_2O, CH_3OH, NH_3 and piperidine. Chem Phys Lett 1988, 144, 317.
94. Kolli, V. S. K.; Orlando, R. A new matrix for matrix-assisted laser desorption/ionization on magnetic sector instruments with point detectors. Rapid Commun Mass Spectrom 1996, 10, 923.
95. Kolli, V. S. K.; Orlando, R. A new strategy for MALDI on magnetic sector mass spectrometers with point detectors. Anal Chem 1997, 69, 327.
96. Kraft, P.; Alimpiev, S.; Dratz, E.; Sunner, J. Infrared, surface-assisted laser desorption ionization mass spectrometry on frozen aqueous solutions of proteins and peptides using suspensions of organic solids. J Am Soc Mass Spectrom 1998, 9, 912.
97. Krause, J.; Stoeckli, M.; Schlunegger, U. P. Studies on the selection of new matrices for ultraviolet matrix-assisted laser desorption/ionization time-of-flight mass-spectrometry. Rapid Commun Mass Spectrom 1996, 10, 1927.
98. Krutchinsky, A. N.; Dolguine, A. I.; Khodorovski, M. A. Matrix-assisted laser desorption/ionization of neutral clusters composed of matrix and analyte molecules. Anal Chem 1995, 67, 1963.
99. Land, C. M.; Kinsel, G. R. Investigation of the mechanism of intracluster proton transfer from sinapinic acid to biomolecular analytes. J Am Soc Mass Spectrom, to appear.
100. Lehmann, E.; Knochenmuss, R.; Zenobi, R. Ionization mechanisms in matrix-assisted laser-desorption/ionization mass-spectrometry—Contribution of preformed ions. Rapid Commun Mass Spectrom 1997, 11, 1483.
101. Lehmann, E.; Vetter, S.; Zenobi, R. Matrix-assisted laser desorption/ionization mass spectra reflect solution phase zinc finger peptide complexation. J Am Soc Mass Spectrom 1999, 10, 000.
102. Lehmann, W. D. Massenspektrometrie in der Biochemie Spektrum; Akadademischer Verlag: Heidelberg, 1996.
103. Li, L.; Wang, A. P. L.; Coulson, L. D. Continuous-flow matrix-assisted laser desorption/ionization mass spectrometry. Anal Chem 1993, 65, 493.
104. Liao, P.–C.; Allison, J. Enhanced detection of peptides in matrix-assisted laser desorption/ionization mass spectrometry through use of charge-localized derivatives. J Mass Spectrom 1995, 30, 511.
105. Liao, P.–C.; Allison, J. Ionization processes in matrix-assisted laser desorption/ionization mass spectrometry: Matrix-dependent formation of $[M + H]^+$ vs $[M + Na]^+$ ions of small peptides and some mechanistic comments. J Mass Spectrom 1995, 30, 408.
106. Lias, S. G. et al. Ionization Energetics Data, NIST Standard Reference Database No. 69, Vol. March; National Institute of Standards and Technology: Gaithersburg, MD 20899 (http://webbok.nist.gov), 1998.

107. Lide, D. R. Handbook of Chemistry and Physics; CRC Press: Boca Raton, 1992.

108. Lidgard, R.; Duncan, M. W. Utility of matrix-assisted laser-desorption/ionization time-of-flight mass-spectrometry for the analysis of low-molecular-weight compounds. Rapid Commun Mass Spectrom 1995, 9, 128.

109. Lindner, B.; Seydel, U. On the influence of laser induced mechanical stress in organic sample layers on the ion formation. In: Ion Formation from Organic Solids: Mass Spectrometry of Involatile Materials; Benninghoven, A. (Ed.); Wiley: Chicester, 1989, 109.

110. Llenes, C. F.; O'Malley, R. M. Cation attachment in the analysis of polystyrene and polyethylene glycol by matrix-assisted laser desorption/ionization mass spectrometry. Rapid Commun Mass Spectrom 1992, 6, 564.

111. Masselon, C.; Salih, B.; Zenobi, R. Matrix-assisted laser desorption/ionization Fourier transform mass spectrometry of luteinizing hormone releasing hormone-metal ion complexes. J Am Soc Mass Spectrom, to appear.

112. McCarley, T. D.; McCarley, R. L.; Limbach, P. A. Electron-transfer ionization in matrix-assisted laser desorption/ionization mass spectrometry. Anal Chem 1998, 70, 4376.

113. Meffert, A.; Grotemeyer, J. Reactions in molecular clusters: Proton transfer to small amino acids. Eur Mass Spectrom 1995, 1, 594.

114. Meffert, A.; Grotemeyer, J. Formation, stability and fragmentation of biomolecular clusters in a supersonic jet investigated with nano- and femtosecond lasers. Ber Bunsenges Phys Chem 1998, 102, 459.

115. Metzger, J. O.; Woisch, R.; Tuszynski, W.; Angermann, R. New type of matrix for matrix-assisted laser desorption mass spectrometry of polysaccharides and proteins. Fresenius J Anal Chem 1994, 349, 473.

116. Mowat, I. A.; Donovan, R. J.; Maier, R. R. J. Enhanced cationization of polymers using delayed ion extraction with matrix-assisted laser desorption/ionization. Rapid Commun Mass Spectrom 1997, 11, 89.

117. Mowry, C. D.; Johnston, M. V. Internal energy of neutral molecules ejected by matrix-assisted laser-desorption. J Phys Chem 1994, 98, 1904.

118. Naven, T. J. P.; Harvey, D. J. Cationic derivatization of oligosaccharides with Girard's T reagent for improved performance in matrix-assisted laser desorption/ionization and electrospray mass spectrometry. Rapid Commun Mass Spectrom 1996, 10, 829.

119. Nelson, C. M. et al. Fragmentation mechanisms of oligonucleotides in MALDI mass spectrometry. SPIE 1996, 2680, 247.

120. Nelson, R. W.; Hutchens, T. W. Mass spectrometric analysis of a transition-metal-binding peptide using matrix-assisted laser-desorption time-of-flight mass spectrometry. A demonstration of probe tip chemistry. Rapid Commun Mass Spectrom 1992, 6, 4.

121. Niu, S.; Zhang, W.; Chait, B. T. Direct comparison of infrared and ultraviolet wavelength matrix-assisted laser desorption/ionization mass spectrometry of proteins. J Am Soc Mass Spectrom 1998, 9, 1.

122. Nordhoff, E. et al. Ion stability of nucleic-acids in infrared matrix-assisted laser-desorption/ionization mass-spectrometry. Nucl Acids Res 1993, 21, 3347.

123. Olumee, Z.; Sadeghi, M.; Tang, X. D.; Vertes, A. Amino-acid-composition and wavelength effects in matrix-assisted laser-desorption/ionization. Rapid Commun Mass Spectrom 1995, 9, 744.

124. Olumee, Z.; Vertes, A. Protonation of glyn homologues in matrix-assisted laser desorption ionization. J Phys Chem B 1998, 102, 6118.

125. Overberg, A.; Hassenbürger, A.; Hillenkamp, F. Laser desorption mass spectrometry. Part II: Performance and applications of matrix-assisted laser desorption/ionization of large biomolecules. In: Mass Spectrometry in the Biological Sciences: A Tutorial; Gross, M. L. (Ed.); Kluwer: Dordrecht, 1992, pp. 181.

126. Overberg, A.; Karas, M.; Bahr, U.; Kaufmann, R.; Hillenkamp, F. Matrix-assisted infrared-laser (2.49 μm) desorption/ionization mass spectrometry of large biomolecules. Rapid Commun Mass Spectrom 1990, 4, 293.

127. Overberg, A.; Karas, M.; Hillenkamp, F. Matrix-assisted laser desorption of large biomolecules with a TEA-CO_2-laser. Rapid Commun Mass Spectrom 1991, 5, 128.

128. Pan, Y.; Cotter, R. J. Measurement of the initial translational energies of peptide ions in laser desorption/ionization mass spectrometry. Org Mass Spectrom 1992, 27, 3.

129. Pieles, U.; Zürcher, W.; Schär, M.; Moser, H. Matrix-assisted laser desorption/ionization time-of-flight mass spectrometry: A powerful tool for the mass and sequence analysis of natural and modified oligonucleotides. Nucl Acid Res 1993, 21, 3191.

130. Preisler, J.; Yeung, E. S. Laser photodissociation of insulin ions generated by matrix-assisted laser-desorption. Anal Chem 1997, 69, 4390.

131. Preston–Schaffter, L. M.; Kinsel, G. R.; Russell, D. H. Effects of heavy-atom substituents on matrices used for matrix-assisted laser-desorption/ionization mass-spectrometry. J Am Soc Mass Spectrom 1994, 5, 800.

132. Puretzky, A. A.; Geohegan, D. B. Gas-phase diagnostics and LIF imaging of 3-hydroxypicolinic acid MALDI matrix plumes. Chem Phys Lett 1997, 286, 425.

133. Quist, A. P.; Huth–Fehre, T.; Sunqvist, B. U. R. Total yield measurements in matrix-assisted laser desorption using a quartz crystal microbalance. Rapid Commun Mass Spectrom 1994, 8, 149.

134. Rashidezadeh, H.; Guo, B. Investigation of metal attachment to polystyrenes in matrix-assisted laser desorption/ionization. J Am Soc Mass Spectrom1998, 9, 724.

135. Riahi, K.; Bolbach, G.; Brunot, A.; Breton, F.; Spiro, M.; Blais, J.–C. Influence of laser focusing in matrix-assisted laser desorption/ionization. Rapid Commun Mass Spectrom.1994, 8, 242.

136. Rockefeller University Web site: http://prowl.rockefeller.edu/cgi-bin/websql/websql.dir/prowl/matrixdepot.hts.

137. Rodgers, M. T.; Armentrout, P. B. Absolute binding energies of lithium ions to short chain alcohols, $C_nH_{2n} + 2O$, n = 1–4, determined by threshold collision-induced dissociation. J Phys Chem 1997, 101, 2614.
138. Salih, B.; Zenobi, R. Matrix-assisted laser desorption/ionization of dye-peptide and dye-protein complexes. Anal Chem 1998, 70, 1536.
139. Schürenberg, M. Matrix-unterstützte Laserdesorptions/Ionisations-Massenspektrometrie (MALDI-MS) in optischer Invertgeometrie und mit Wellenlängen im sichtbaren Spektralbereich. Ph. D. Thesis, Westfälische Wilhelms–Universität Münster, Münster, 1996, p. 175.
140. Scott, C. T. J.; Kosmidis, C.; Jia, W. J.; Ledingham, K. W. D.; Singhal, R. P. Formation of atomic hydrogen in matrix-assisted laser desorption/ionization. Rapid Commun Mass Spectrom 1994, 8, 829.
141. Spengler, B.; Bökelmann, V. Angular and time-resolved intensity distributions of laser-desorbed matrix ions. Nucl Instr Meth Phys Res B 1993, 82, 379.
142. Spengler, B.; Karas, M.; Bahr, U.; Hillenkamp, F. Excimer laser desorption mass spectrometry of biomolecules at 248 and 193 nm. J Phys Chem 1987, 91, 6502.
143. Spengler, B.; Kaufmann, R. Gentle probe for tough molecules: Matrix-assisted laser desorption mass spectrometry. Analusis 1992, 20, 91.
144. Spengler, B.; Kirsch, D.; Kaufmann, R. Fundamental aspects of postsource decay in matrix-assisted laser desorption mass spectrometry. J Phys Chem 1992, 96, 9678.
145. Spengler, B. et al. Peptide sequencing of charged derivatives by postsource decay MALDI mass spectrometry. Int J Mass Spectrom Ion Proc 1997, 169/170, 127.
146. Standing, K. G.; Ens, W. Methods and mechanisms for producing ions from large molecules; Plenum: New York & London, 1996.
147. Steenvoorden, R. J. J. M.; Breuker, K.; Zenobi, R. The gas-phase basicity of MALDI matrices. Eur Mass Spectrom 1997, 3, 339.
148. Strahler, J. R.; Smelyanskiy, Y.; Lavine, G.; Allison, J. Development of methods for the charge derivatization of peptides in polyacrylamide gels and membranes for their direct analysis using matrix-assisted laser desorption/ionization mass spectrometry. Int J Mass Spectrom Ion Proc 1997, 169/170, 111.
149. Sunner, J. Ionization in liquid secondary ion mass spectrometry (LSIMS). Org Mass Spectrom 1993, 28, 805.
150. Sunner, J.; Dratz, E.; Chen, Y. Graphite surface-assisted laser desorption/ionization time-of-flight mass spectrometry of peptides and proteins from liquid solutions. Anal Chem 1995, 67, 4335.
151. Sunner, J. A.; Kulatunga, R.; Kebarle, P. Fast atom bombardment mass spectrometry and gas-phase basicities. Anal Chem 1986, 58, 1312.
152. Sze, E. T. P.; Chan, T.–W. D.; Wang, G. Formulation of matrix solutions for use in matrix-assisted laser desorption/ionization of biomolecules. J Am Soc Mass Spectrom 1998, 9, 166.
153. Szekely, G. Mechanisms of ion formation and fragmentation by fast-atom bombardment and matrix-assisted laser desorption/ionization mass spectrometry. Ph. D. Thesis, Mich State U, East Lansing, MI, 1997, p. 164.
154. Taft, R. W.; Topsom, R. D. The nature and analysis of substituent effects. Prog Phys Org Chem 1987, 16, 1.
155. Tanaka, K.; Waki, H.; Ido, Y.; Akita, S.; Yoshida, Y.; Yoshida, T. Protein and polymer analyses of up to m/z 100,000 by laser ionization time-of-flight mass spectrometry. Rapid Commun Mass Spectrom 1988, 2, 151.
156. Tang, W.; Nelson, C. M.; Zhu, L.; Smith, L. M. Positive-ion formation in the ultraviolet matrix-assisted laser desorption/ionization analysis of oligonucleotides by using 2,5-dihydroxybenzoic acid. J Am Soc Mass Spectrom 1997, 8, 218.
157. Tang, X.; Sadeghi, M.; Olumee, Z.; Vertes, A. Matrix-assisted laser desorption/ionization by two collinear subthreshold laser pulses. Rapid Commun Mass Spectrom 1997, 11, 484.
158. van der Peyl, G. J. Q.; Isa, K.; Haverkamp, J.; Kistemaker, P. G. Gas-phase ion/molecule reactions in laser desorption mass spectrometry. Org Mass Spectrom 1981, 16, 416.
159. Vertes, A.; Irinyi, G.; Gijbels, R. Hydrodynamic model of matrix-assisted laser desorption mass spectrometry. Anal Chem 1993, 65, 2389.
160. von Helden, G.; Wyttenbach, T.; Bowers, M. T. Conformation of macromolecules in the gas phase: Use of matrix-assisted laser desorption methods in ion chromatography. Science 1995, 267, 1483.
161. Wang, B. H.; Dreisewerd, K.; Bahr, U.; Karas, M.; Hillenkamp, F. Gas-phase cationization and protonation of neutrals generated by matrix-assisted laser desorption. J Am Soc Mass Spectrom 1993, 4, 393.
162. Westman, A.; Huth–Fehre, T.; Demirev, P.; Bielawski, J.; Medina, N.; Sundqvist, B. U. R. Matrix-assisted laser-desorption/ionization: Dependence of the ion yield on the laser beam incident angle. Rapid Commun Mass Spectrom 1994, 8, 388.
163. Williams, J. B.; Gusev, A. I.; Hercules, D. M. Use of liquid matrices for matrix-assisted laser desorption/ionization of polyglycols and poly(dimethylsiloxanes). Macromolec 1996, 29, 8144.
164. Wong, C. K. L.; Chan, T. W. D. Cationization processes in matrix-assisted laser desorption/ionization mass-spectrometry—Attachment of divalent and trivalent metal ions. Rapid Commun Mass Spectrom 1997, 11, 513.
165. Woods, A. S.; Buchsbaum, J. C.; Worall, T. A.; Berg, J. M.; Cotter, R. J. Matrix-assisted laser desorption/ionization of noncovalently bound compounds. Anal Chem 1995, 67, 4462.
166. Wu, K. J.; Odom, R. W. Matrix-enhanced secondary-ion mass spectrometry—A method for molecular analysis of solid-surfaces. Anal Chem 1996, 68, 873.
167. Wu, K. J.; Shaler, T. A.; Becker, C. H. Time-of-flight mass-spectrometry of underivatized single-stranded-DNA oligomers by matrix-assisted laser-desorption. Anal Chem 1994, 66, 1637.
168. Wu, K. J.; Steding, A.; Becker, C. H. Matrix-assisted laser desorption time-of-flight mass spectrometry of oligonucleo-

tides using 3-hydroxypicolinic acid as an ultraviolet-sensitive matrix. Rapid Commun Mass Spectrom 1993, 7, 142.

169. Wu, Z.; Fenselau, C. Proton affinities of polyglycines assessed by using the kineteic method. J Am Soc Mass Spectrom 1992, 3, 863.
170. Wu, Z.; Fenselau, C. Structural determinants of gas-phase basicities of peptides. Tetrahedron 1993, 49, 9197.
171. Yau, P. Y.; Chan, T. W. D.; Cullis, P. G.; Colburn, A. W.; Derrick, P. J. Threshold fluences for production of positive and negative ions in matrix-assisted laser desorption/ionization using liquid and solid matrices. Chem Phys Lett 1993, 202, 93.
172. Yong, H.; Russell, D. H. Photochemistry and proton transfer reaction chemistry of selected cinnamic acid derivatives in hydrogen bonded environments. Int J Mass Spectrom Ion Proc 1998, 175, 187.
173. Yong, H. Photoinduced proton transfer in supersonic expansion and its relevance to matrix-assisted laser desorption/ionization (MALDI). Ph. D. Thesis, Texas A&M U, College Station, TX, 1998,
174. Zenobi, R. Laser-assisted mass spectrometry. Chimia 1997, 51, 801.
175. Zhang, W.; Niu, S.; Chait, B. T. Exploring infrared wavelength matrix-assisted desorption/ionization of proteins with delayed extraction time-of-flight mass spectrometry. J Am Soc Mass Spectrom 1998, 9, 879.
176. Zhao, S. et al. Novel method for matrix-assisted laser mass spectrometry of proteins. Anal Chem 1991, 63, 450.
177. Zhigilei, L. V.; Garrison, B. J. Velocity distributions of molecules ejected in laser ablation. Appl Phys Lett 1997, 71, 551.
178. Zhigilei, L. V.; Garrison, B. J. Velocity distributions of analyte molecules in matrix-assisted laser desorption from computer simulations. Rapid Comm Mass Spectrom 1998, 12, 1273.
179. Zhigilei, L. V.; Kodali, P. B. S.; Garrison, B. J. Molecular dynamics model for laser ablation and desorption of organic solids. J Phys Chem B 1997, 101, 2028.
180. Zhou, J.; Ens, W.; Standing, K. G.; Verentchikov, A. Kinetic energy measurement of molecular ions ejected into an electric field by matrix-assisted laser desorption. Rapid Commun Mass Spectrom 1992, 6, 671.
181. Zhu, L.; Parr, G. R.; Fitzgerald, M. C.; Nelson, C. M.; Smith, L. M. Oligodoxynucleotide fragmentation in MALDI/TOF mass spectrometry using 355-nm radiation. J Am Chem Soc 1995, 117, 6048.
182. Zhu, Y. F.; Lee, K. L.; Tang, K.; Allman, S. L.; Taranencko, N. I.; Chen, C. H. Revisit of MALDI for small proteins. Rapid Commun Mass Spectrom 1995, 9, 1315.
183. Zöllner, P.; Schmid, E. R.; Allmaier, G. $K_4(Fe(CN)_6$/glycerol—A new liquid matrix system for matrix-assisted laser desorption/ionization mass spectrometry of hydrophobic compounds. Rapid Commun Mass Spectrom 1996, 10, 1278.
184. Zöllner, P.; Stübinger, G.; Schmid, E.; Pittenauer, E.; Allmaier, G. MALDI mass spectrometry of biomolecules and synthetic polymers using alkali hexacyanoferrate (II) complexes and glycerol as a matrix. Int J Mass Spectrom Ion Proc 1997, 169/170, 99.